Diversity in Sedimentary Organic Matter along the River-Aquifer Interface and its Implications on Arsenic Mobility: the Meghna River Corridor in Bangladesh

Thomas S. Varner[1*], Harshad V. Kulkarni[1,4*], M. Bayani Cardenas[2], Peter S.K. Knappett[3], Saugata Datta[1*]

[1]Department of Earth and Planetary Sciences, University of Texas at San Antonio, San Antonio, TX, 78249, USA
[2] Department of Geological Sciences, The University of Texas at Austin, TX 78712, USA
[3] Department of Geology and Geophysics, Texas A&M University, College Station, TX 77843, USA
[4] School of Civil and Environmental Engineering, Indian Institute of Technology Mandi, Himachal Pradesh, 175005, India.

Corresponding authors: Thomas S. Varner (tom.varner@my.utsa.edu), Harshad V. Kulkarni (harshad@iitmandi.ac.in / harshad.env@gmail.com), Saugata Datta (saugata.datta@utsa.edu)

Highlights

1. Infrared spectroscopic analyses of sedimentary organic matter (SOM) from arsenic contaminated river-aquifer interface.
2. Enrichment of polysaccharide and carbonyl functional groups in near-surface silt layer
3. Enrichment of carboxyl function groups in underlying clay aquitard
4. Distribution of organic functional groups provides insights on mobilization and sequestration of arsenic in the aquifer-river mixing zone
5. Clay aquitard SOM contained abundant carboxylate groups which favor complexation with Fe and As
6. Reduction of Fe-oxides in the riverbank is sustained by the reactive nature of the near-surface silt SOM

Keywords: Sedimentary Organic Matter; Arsenic; Hyporheic zone; Functional groups; Meghna River; Fourier Transform Infrared Spectroscopy.

Graphical Abstract

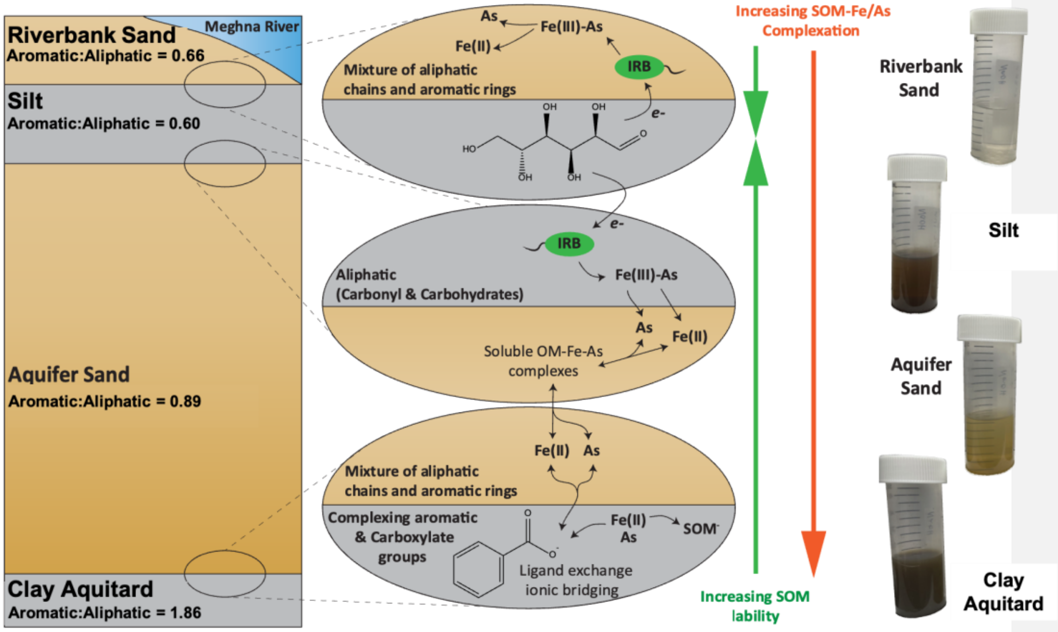

Abstract

The presence and character of sedimentary organic matter (SOM) regulates the mobility of arsenic (As) as labile SOM determines redox reactions and zonation. Near rivers, the hyporheic zone (HZ) of oxic river water and anoxic regional groundwater may lead to the production (or dissolution) of iron (Fe)-oxides which are capable of sequestering (and mobilizing) As depending on dynamic redox conditions. This study characterizes the chemical reactivity of SOM from HZ sediments along the Meghna River in Bangladesh, and an adjacent As-contaminated shallow (< 50 m) alluvial aquifer. The SOM in both the riverbank and aquifer is primarily composed of terrestrially-derived humic-like organic matter; however, the distribution of organic functional groups varies with the type of subsurface sediments. A shallow silt layer (~3 m below ground level) within the sandy aquifer contains fresher SOM, potentially of microbial origin, with higher proportions of amides and more labile polysaccharide moieties. On the contrary, SOM in an underlying clay aquitard (~37 m below ground) contains older, more recalcitrant, terrestrially-derived material with high proportions of aromatic carboxylate functional groups. The labile SOM from the silt layer supports the microbially mediated reductive dissolution of As-bearing Fe-oxides, preventing the accumulation of As in the HZ. The carboxylate-rich SOM in the clay aquitard helps maintain groundwater As concentrations by favoring the formation of soluble Fe and As complexes. These findings suggest that the SOM within the Meghna Riverbank and its adjacent aquifer contain differing reactive properties that likely influence the geochemical processes governing As and Fe mobility.

1 Introduction

Organic matter in sediments, sedimentary organic matter (SOM), is known to play a vital role in mobilizing arsenic (As) from shallow Holocene aquifers in the Ganga-Meghna-Brahmaputra (GMB) delta in south Asia (Nickson et al., 2000; McArthur et al., 2004; Mladenov et al., 2010; Mailloux et al., 2013). Elevated As concentrations in groundwater in the aquifers of the GMB delta jeopardize the health of millions who rely on the groundwater for drinking purposes (Flanagan et al., 2012). Indeed, exposure to groundwater As exceeding the World Health Organization (WHO) maximum contaminant level of 10 µg/L in Bangladesh has been of global concern for decades leading to many studies which have improved the understanding of the natural processes promoting high groundwater As in reducing fluvio-deltaic aquifers (Smith et al., 2000; BGS&DPHE, 2001; Mukherjee & Bhattacharya, 2001; Yu et al., 2003; Flanagan et al., 2012). Yet reliance on elevated groundwater that is high in As is a continuing struggle for many in the Bengal basin and the heterogeneous modes of As mobilization leading to contaminated groundwater are not fully understood. A key reaction that releases As to pore-waters is the microbially mediated reductive dissolution of As-bearing Iron (Fe)-oxy(hydro)oxide minerals in the presence of labile organic matter (OM) (Nickson et al., 1998; Nickson et al., 2000; Bhattacharya et al., 2001; McArthur et al., 2001; Zheng et al., 2004; Hasan et al., 2007; Glodowska et al., 2020; Qiao et al., 2020; Vega et al., 2020). However, in natural settings where a wide range of geochemical conditions exist in close proximity, various process may contribute to As mobilization simultaneously (Nicholas et al., 2017). For example, As mobility can be exacerbated by competition for sorption sites between As and dissolved silica (Smedley & Kinniburgh, 2002; Waltham & Eick, 2002; Harvey et al., 2005), carbonate (Appelo et al., 2002; Harvey et al., 2002; Biswas et al., 2011), phosphate (Redman et al., 2002; Simeoni et al., 2003; Bauer & Blodau, 2006;

Gustafsson, 2006; Wang & Mulligan, 2006; Xue et al., 2019), and OM (Redman et al., 2002; Simeoni et al., 2003; Bauer & Blodau, 2006; Gustafsson, 2006; Wang & Mulligan, 2006; Xue et al., 2019). Regardless of the precise mechanism of As mobilization, it is clear that OM plays a ubiquitous role in regulating groundwater As concentrations in alluvial aquifers and may be key to predicting the distribution of As (Anawar et al., 2003; Mladenov et al., 2010; Anawar et al., 2013).

Organic matter is known to participate in variety of chemical reactions in the environment. It has a significant electron donating capacity which helps create reducing conditions when it undergoes aerobic oxidation (Aeschbacher et al., 2010; Macalady & Walton-Day, 2011; Wallace et al., 2017; Lv et al., 2018) and alters the surface reactivity of minerals (Qu & Cwiertny, 2013). As a result, OM participates in the geochemical cycling of both major and trace metals (Li et al., 2013; Mostofa et al., 2013). In fact, over 20% of OM in both terrestrial and oceanic sediments is associated with and stored in reactive Fe minerals (Wagai & Mayer, 2007; Lalonde et al., 2012). The composition of OM varies widely among sources in nature, with, various proportions of microbial products, humic and fulvic acids, and humin. Most OM is generated largely as the result of biological metabolism (Laspidou & Rittmann, 2002). In general, the majority of OM is composed of refractory humic substances (i.e. humic acid, fulvic acid and humin) (Piccolo, 1996; Senesi et al., 2003) and labile OM which consists of sugars, carbohydrates, and protein-like components (i.e. amino acids) (Coble & Timperman, 1998; Yamashita & Tanoue, 2003; Borisover et al., 2012). Together, these refractory and labile OM components drive the net heterotrophy in the environment (McManus et al., 2003). Humic substances typically contain large proportions of carboxylate functional groups which form strong complexes with metal cations (Fe^{3+} and Al^{3+}) via ligand exchange or cationic bridging and have been implicated in adsorption reactions of As on the surface of Fe-OM complexes (Deng & Dixon, 2002; Sharma et al., 2010; Liu et al., 2011). These carboxyl-metal complexes may either stabilize and preserve the OM and Fe in the sediments (Curti et al., 2021), or if the SOM contains high amounts of carboxylic acids, solubility increases promoting the mobility of Fe-OM-As complexes (Ni & Pignatello, 2018; Zhang et al., 2021). In contrast, the labile pool of OM comprised of protein-like compounds and microbial byproducts which are readily biodegradable, provides accessible electrons as a preferred energy source for microbial respiration (Haynes, 2005). Due to the heterogeneous composition of OM, the mechanisms provided by OM to As mobilization, whether from complexation (Sharma et al., 2010; Liu et al., 2011; Liu et al., 2020b), electron shuttling promoting microbially driven reduction (Lovley et al., 1996; Scott et al., 1998; Kappler et al., 2004; Sposito, 2011; Kulkarni et al., 2018b; Yi et al., 2019; Qiao et al., 2020; Wang et al., 2020; Qiao et al., 2021; Li et al., 2022), or competition for sorption sites (Bauer & Blodau, 2006), depends largely on the chemical makeup of the source OM.

The reactivity of OM is mostly determined by its original source, yet the relative importance of the different sources of OM driving As mobilization in the aquifers of Bangladesh remains uncertain (Mailloux et al., 2013). A few hypotheses have been put forward regarding the source of OM in the aquifers, including: downward infiltration of dissolved OM from surface water (Harvey et al., 2006; Neumann et al., 2010), buried silt, peat, or clay lenses (McArthur et al., 2001; McArthur et al., 2004; Ravenscroft et al., 2005), and from OM dispersed within the aquifer sediments (Datta et al., 2011; Neumann et al., 2014). Considering that OM drives As mobilization in the aquifers of Bangladesh, it is imperative to comprehensively understand the nature of the SOM. Also considering that OM has an affinity for Fe-oxides, areas where abundant Fe^{III} and reactive SOM co-occur, such as redox interfaces, are likely key locations where As is both trapped and mobilized under the influence of SOM. Ultimately, the geochemical cycling of OM, Fe, and As are integrally related and redox interfaces have been implicated in acting as intermediate barriers that limit the transportation of both inorganic and organic constituents (Charette & Sholkovitz, 2002; Datta et al., 2009; Riedel et al., 2013).

The hyporheic zone (HZ) represents a redox transition zone along the river where oxic river water and reducing groundwater mix to form a biogeochemical hotspot with enhanced chemical reaction rates relative to the adjacent areas (McClain et al., 2003). Redox conditions throughout the HZ support a wide array of microbial communities which may effectively metabolize OM from the river, groundwater, and sediments, which impacts Fe cycling and ultimately regulates the attenuation of both organic and inorganic contaminants (Fiebig, 1995; Findlay et al., 2003; Fischer et al., 2005; Nogaro et al., 2013; Shuai et al., 2017a; Zhu et al., 2020; Xia et al., 2023). One such feature likely present in HZs, termed a natural reactive barrier (NRB) (Bone et al., 2006), removes As when amorphous Fe-oxides precipitate on mineral surfaces along the surface water-groundwater interface from the interaction between the oxic surface water and reduced Fe-rich groundwater (Charette & Sholkovitz, 2002; Charette et al., 2005; Bone et al., 2006; Charette & Sholkovitz, 2006; Jung et al., 2009). Evidence of a seasonal HZ NRB has been observed along the tidally influenced Meghna River in Bangladesh during the dry season when the reduced groundwater is drawn towards the river (Datta et al., 2009; Jung et al., 2012; Jung et al., 2015; Berube et al., 2018; Varner et al., 2022), which then interacts with infiltrating oxic river water to precipitate amorphous Fe-oxides capable of sequestering large amounts of As (Datta et al., 2009; Jung et al., 2015; Berube et al., 2018; Huang et al., 2022). Although the response of a NRB to changing redox conditions has not been examined, Fe-oxides in the HZ may be dissolved under reducing conditions introduced by either rapid groundwater discharge in the early dry season

(Datta et al., 2009; Baken et al., 2015; Berube et al., 2018) or from the inundation and seasonal deposition of Fe-OM rich-sediment during the wet season (Stahl et al., 2016; Wallis et al., 2020). Nevertheless, the ability of OM to provide energy for microbial reduction of Fe-oxides and form As and Fe complexes makes the characterization of OM a necessary component in defining the behavior of As across redox interfaces.

Prior work along the Meghna River indicated that surficial sand layers promote the formation of a NRB whereas surficial silt layers inhibit the mixing required to generate a Fe-oxide-rich NRB (Jung et al., 2015). Pedrazas et al. (2021) determined the presence of buried silt layer (~ 3 to 7 m bgl) at the present site using geophysical measurements. Our recent work at this site along Meghna River in Bangladesh (Varner et al., 2022) showed that the riverbank sediments contained low concentrations of As compared to prior work that reported Fe and As enrichment within the Meghna River HZ (Datta et al., 2009; Jung et al., 2012; Jung et al., 2015; Berube et al., 2018). Such low As in the HZ sediments at this site may be attributed to the buried silt layer that may prevent Fe-oxide formation by impeding groundwater mixing or providing OM to the riverbank to sustain reducing conditions. The water-extractable SOM from the riverbank sand, buried silt layer, aquifer sand, and underlying clay aquitard showed distinct fluorescence signatures (Varner et al., 2022), suggesting that the buried silt layer may be providing sufficient labile organic matter for heterotrophic metabolisms. Therefore, we hypothesized that such optically distinct SOM in the subsurface layers at our site may contain chemical distinct organic functional groups, and its detailed characterization will help in explaining the role of SOM in mobility of As and Fe within HZ of the Meghna River.

To our knowledge the relationship between the specific chemical composition of OM within riverbank sediments and As mobilization has not yet been extensively studied in the Bengal basin.

In this study, we define the structural characteristics of SOM at selected and previously well-characterized locations from the As contaminated aquifer and the adjacent HZ sediments along the Meghna River utilizing both UV-Vis and FTIR spectroscopic techniques (Minor et al., 2014). The specific functional groups comprising the SOM helped to characterize the reactivity of SOM and its relationship to As mobilization in the aquifer and riverbank HZ sediments.

2 Methods

2.1 Study site

The study site lies along the Meghna River 30 km east of Dhaka, adjacent to the village of Nayapara (23.7°N, 90.7°E) within the Narayanganj district (Fig. 1). The lithology of shallow aquifers (<60 m) in the region are typical of fluvio-deltaic depositional environments, consisting of medium to fine unconsolidated sand with interbedded lenses of silt and clay (Aziz et al., 2008; Bibi et al., 2008; Weinman et al., 2008). The detailed lithology at this site along the Meghna River is described in Varner et al. (2022). Briefly, it consists of four units; an underlying clay layer at ~36 m below ground level (bgl) overlain by medium sands which comprises the shallow aquifer between 36 and 7 bgl. This aquifer is overlain by a silt layer between 7 and 3 m bgl; this silt layer is overlain by fine sand between 3 and 0 m bgl.

The co-occurrence of high dissolved As and Fe concentrations in the nearby shallow aquifers of the Meghna River floodplain have been well documented (BGS&DPHE, 2001; van Geen et al., 2003; van Geen et al., 2014). Along the Meghna River shallow groundwater flows towards the river for most of the year (Huang et al., 2022), and multiple studies have observed very high solid-phase concentrations of As (>100 mg/kg) and Fe (>30,000 mg/kg) within the HZ sediments (Datta et al., 2009; Jung et al., 2012; Jung et al., 2015; Berube et al., 2018). This suggests that advected As and Fe from the shallow aquifer may accumulate in the HZ under the influence of mixing with

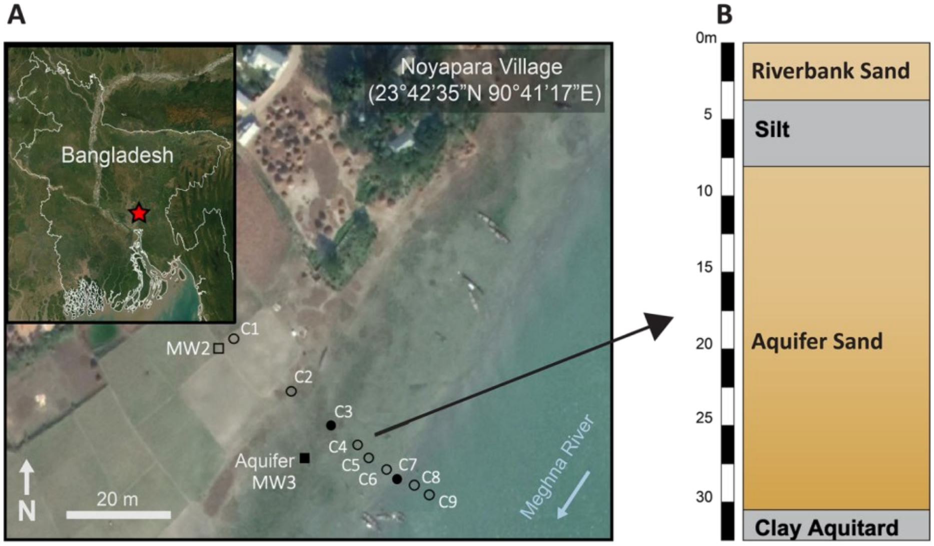

Figure 1. (A) Map of study site with sampling locations of riverbank sediment (circles) and aquifer sediment (squares). The filled symbols represent the sampling locations of the sediment used in this study. (B) Depiction of the subsurface lithology at the site derived from an electrical resistivity transect along the riverbank and drill cuttings from the aquifer borehole (Pedrazas et al., 2021; Varner et al., 2022).

the oxygenated river water. This mixing is in turn driven by tidal and seasonal fluctuations in the river stage (Shuai et al., 2017b). During the dry season, the river is most strongly gaining. However, when the riverbank becomes inundated during the wet season, the river is weakly gaining or slightly losing (Berube et al., 2018).

2.2 Sample collection and analyses

The riverbank and aquifer sediment samples used in this study (n = 8) were collected from the study site along the Meghna River in January 2020. The aquifer sediment was collected as sediment cuttings from a borehole installed using the traditional hand flapper method (n = 6) (Horneman et al., 2004), whereas the riverbank sediment (n = 2) was collected from a depth of 0.6 m bgl using a direct push sediment probe (AMS Inc., USA). Four representative samples from riverbank sand (RBS, 0.6 m), buried silt (SLT, 6 m), aquifer sand (AQS, 23 m), and underlying clay aquitard (CLY, 37 m) were selected for this study. Analyses of RBS (n = 32, from nine sediment cores), AQS (n = 13), SLT (n = 3), and CLY (n = 2) samples from three drill cuttings (Varner et al., 2022) showed that the optical properties of water-extractable SOM were similar within the sample groups (e.g., RBS, AQS, SLT and CLY) but distinct from each other. We therefore selected four well-characterized samples from each group (RBS, SLT, AQS and CLY) for the detailed functional group characterization, whose elemental composition, particle size distribution, and optical properties of water-extractable organic matter were described in Varner et al. (2022). All sediment samples used in this study were stored in Mylar Remel® bags with an O_2 absorbent pouch and kept at -7 °C until analysis.

2.3 Sedimentary organic matter (SOM) extraction using NaOH

To extract the SOM from the riverbank and aquifer sediments, 2.5 g of air-dried sediment was powdered using an agate mortar and pestle and placed in a 50 ml centrifuge tube with 25 ml of 0.1 M NaOH solution (pH = 10.6). The mixture was mechanically shaken for 20 h (table shaker, 60 rpm) at ambient temperature. The supernatant was separated from the solid phase by centrifugation (12,000 rpm, 20 min). Extractions using a dilute NaOH solution have been widely used to extract natural SOM (Stevenson, 1994). Further acidification, following the NaOH solution, allows for the partitioning of humic and fulvic acids (Bai et al., 2020). In this study, the extract solutions were not acidified in order to retain all humic and non-humic fractions of SOM. Such NaOH extractions have been shown to release a large percentage of the SOM and include not only humic substances, but also the low molecular weight acids, protein-like substances, and saccharide derivatives which comprise between 25-35% of the overall SOM in inorganic soils (Schnitzer, 1983; Ping et al., 2001). Following centrifugation, the supernatant of the NaOH extractant solution was 0.45 μm filtered and immediately lyophilized for FTIR measurement to avoid any loss or degradation of the OM in solution (Lin, 2015; Sandron et al., 2015).

2.4 Spectroscopic characterization of NaOH extractable organic matter

The mid-infrared spectra of the lyophilized NaOH sediment-extracts and a standard humic acid (HA) material (Sigma Aldrich humic acid, Aldrich Chemical Co., Product No. H16752) were obtained by attenuated total reflectance Fourier-transform infrared spectroscopy (ATR-FTIR) over the 4000-650 cm^{-1} range on a Shimadzu IRSpirit spectrometer (Shimadzu Corporation, Japan). The spectrometer was fitted with a QATR-S diamond crystal attachment and a germanium-coated KBr beam splitter. Data were obtained as absorbance [log(1/reflectance)] and 64 scans at a resolution of 4 cm^{-1} were averaged to obtain each sample spectrum. Background readings were collected between samples and subtracted from the subsequent measurements. The collected FTIR spectra were processed, baseline corrected, and smoothed in Spectragryph (v1.2.16.1).

To further characterize the spectroscopic properties of SOM, simultaneous UV-Vis measurement of the absorbance between 240 and 450 nm and the fluorescence between 300 and 600 nm was collected on the extract solutions using a benchtop fluorometer (Aqualog, Horiba). Following the methods described in Kulkarni et al. (2017), the spectroscopic data from the absorbance and fluorescence wavelengths were used to generate an excitation-emission matrix (EEM) for each sample. Specific parameters were calculated from the UV-Vis spectroscopic data to provide further characterization of the source and dynamic processes of the SOM and are detailed in the supplementary text 2. Furthermore, the assignment of peaks at established excitation/emission (ex/em) pairs for the peak-picking method is useful for characterizing and monitoring the organic properties in spectroscopic data (Goldman et al., 2012; Chen & Yu, 2021). For this study, commonly used ex/em pairs in the fluorescence spectra which reflect the structures present in the OM were used, including humic-like (peak A, 260/380 – 460), fulvic-like (peak C, 320 – 260/420 – 460), microbially derived (peak M, 290 – 310/370 – 410), protein-like tryptophan (peak T, 270/340), and protein-like tyrosine (peak B, 270/305) (Coble et al., 1998; Coble et al., 2014).

The drEEM toolbox (v 0.6.0) (Murphy et al., 2013) was used for parallel factor analysis (PARAFAC) modeling of a 96 sample dataset of fluorescence spectra comprised of the samples obtained in this study and a previous dataset which included groundwater, riverbank porewater, river water, and sediment-water extracts from the same location (Table S1) (Varner et al., 2022). The EEMs included in the PARAFAC model were corrected to account for scatter, anomalies, and artifacts during collection of the spectra. Out of an initial 97 samples, only 1 sample was identified as an outlier with a leverage value nearing 1, indicating a high degree of deviation from the average distribution, and was removed from the model due to this analytical error. The remaining 96 samples produced a three-component model and was validated by a split-half analysis of 50 models with three components, which confirmed the reliability of the three-component model through random initialization techniques.

3 Results

3.1 Functional group assignments and variations in SOM

The FTIR spectra provided diagnostic information on the functional groups present in the SOM. The assignment of functional groups was performed by comparing the sample spectra to previously reported ranges for common functional groups in natural waters and sediments (Table 1), as well as utilizing co-occurring signals in the spectra that are associated with specific functional groups (i.e., aliphatic CH shows peaks at both ~1450 cm^{-1} for deformation and ~2920 cm^{-1} for stretching). The possible effects from alkaline extraction on the SOM were also considered for the assignment of functional groups in the spectra. A more detailed description of peak assignments is provided in the supplementary text.

The FTIR spectra of the lyophilized NaOH extracts were compared to a standard humic acid (HA) (Fig. 2a). The HA displayed prominent peaks at ~3400, 1590, 1390, and between 1100-1030 cm^{-1}, which are typical for Sigma Aldrich HA, and are attributed to O—H stretches, aromatic C═C stretching, symmetric C—O stretching of carboxylic groups, and polysaccharide moieties, respectively (Guan et al., 2006; Liu et al., 2015). Based upon the peak assignments and known structure of the functional groups (Table 1) (Li et al., 2015), the aromaticity (a measurement of molecules that are both cyclic and planar) of the Sigma Aldrich HA was determined to be 56%, which is consistent with previously reported values (Kobayashi & Sumida, 2015) and is comparable to that of the ^{13}C nuclear magnetic resonance estimates for the International Humic Substances Society's standard HA (Thorn et al., 1989). The aromaticity of the SOM in the samples ranged between 40-65%. Overall, the FTIR spectra for the NaOH extracts show IR absorptions that are typical for alkaline soil extracts (Oren & Chefetz, 2012). For comparison of relative peak sizes, normalized FTIR spectra are shown in Figure S1.

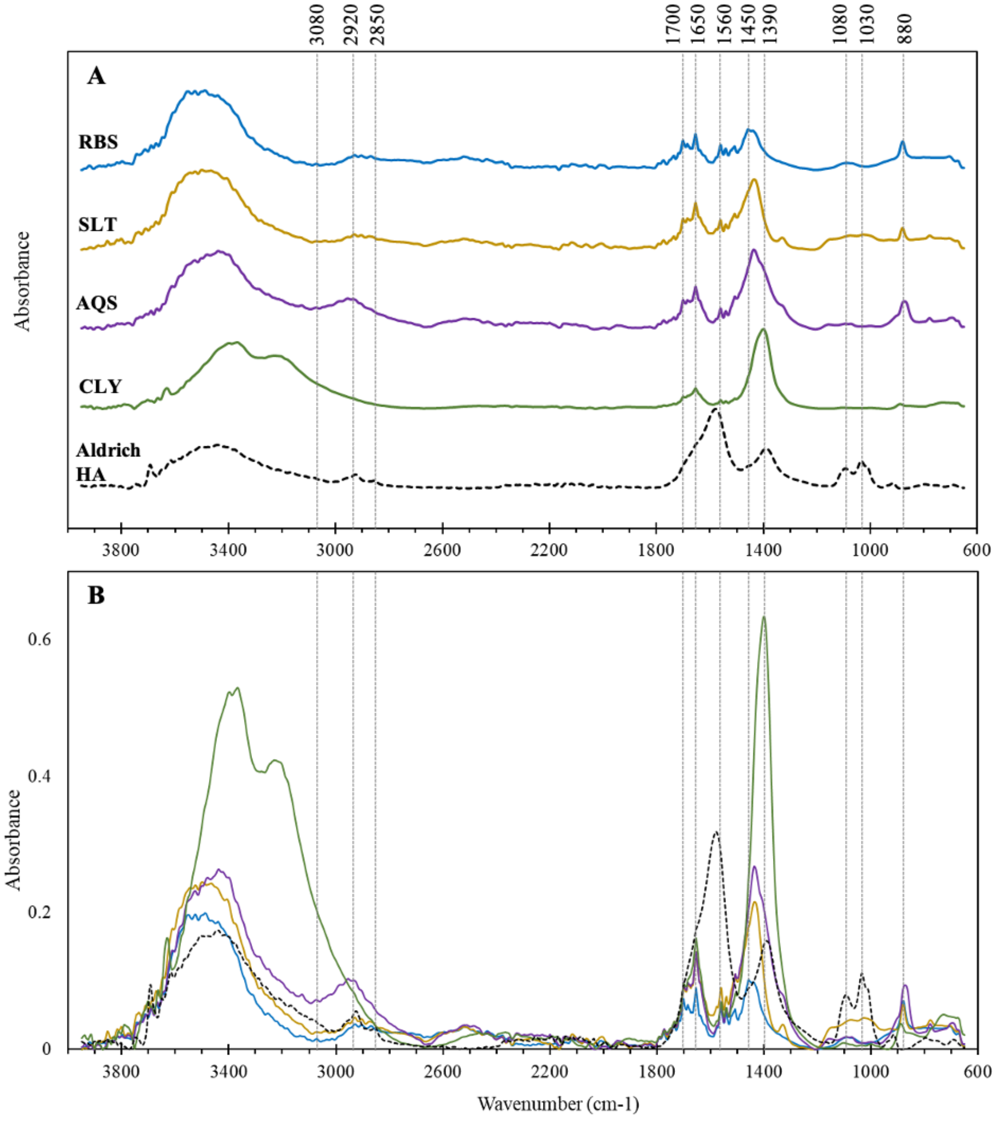

Figure 2. FTIR spectra of the lyophilized NaOH sediment extracts and Sigma Aldrich humic acid with stacked spectra (A) and a panel showing all sample spectra together for comparison of peak intensities among samples (B). The riverbank sand, silt, aquifer sand, and the clay aquitard are denoted by RBS, SLT, AQS, and CLY, respectively.

286

Table 1. Functional group assignments for specific bands and peaks observed within the mid-infrared wavelengths.

Absorption (cm^1)	**FTIR band**	**Assignment**	**Reference**
3700-3300	O—H bonds	Unresolved: phenol, alcohol, carbohydrates, COOH, Si—O—H in clay minerals, N—H stretch	1-15
3100-3030	Aromatic C—H stretch	Aromatic stretch of highly substituted rings in HA macromolecules	1, 2, 5, 9, 12, 16
2970-2820	Aliphatic C—H Stretch	Aliphatic C—H stretch of CH_2	1-13, 16-20
1720-1700	C═O stretch	Protonated carboxylic acid: aliphatic	2-4, 6, 7, 10-15, 18, 19, 21-25
1670-1630	C═O stretch	Aliphatic carbonyl structures including proteinaceous amide I, conjugated ketones, and quinone-like compounds	1-7, 9-11, 13-15, 18-25
1630-1600	Aromatic C═C stretch	Aromatic ring stretch. May indicate ternary As-Fe-OM complexes	3-8, 10, 15, 19, 20
1570-1550	Aromatic C═C stretch	Possible contribution from asymmetric COO^- stretches	1-3, 8, 15, 16, 23, 26
1515-1490	Aromatic C═C stretch	Possible contribution of amide II and peptide	1, 4, 5, 7-11, 15, 16, 18-20, 23
1470-1430	C—H deformation	Aliphatic C—H deformation	1, 2, 4, 5-9, 14-19, 21-23, 26
1420-1370	Symmetric C—O Stretch	Aromatic carboxylate derivatives. Indicative of Na^+ salts (i.e., sodium benzoate)	1, 5-7, 11, 15, 17-19, 21-27
1185-975	C—O—C and C—O—H stretching	Carbohydrates: aliphatic polysaccharide moieties	2, 4, 5-8, 11, 15, 19, 20, 26
900-860	C—H out-of-plane bend	C—H bend of aromatic rings	1, 3, 5, 9, 15, 17, 18, 20, 23

1. Bellamy (2013) **2.** de Melo Benites et al. (2005) **3.** Fultz et al. (2014) **4.** Fernández-Getino et al. (2010) **5.** Senesi et al. (2003) **6.** Olk et al. (2000) **7.** Chefetz et al. (1998) **8.** Sánchez-Monedero et al. (2002) **9.** Tatzber et al. (2007) **10.** MacCarthy and Rice (1985) **11.** Lumsdon and Fraser (2005) **12.** Mecozzi and Pietrantonio (2006) **13.** Litvin and Minaev (2013) **14.** Reddy et al. (2018) **15.** Minor and Stephens (2008) **16.** Bustin and Guo (1999) **17.**Oren and Chefetz (2012) **18.** Nuzzo et al. (2020) **19.** Guggenberger et al. (1994) **20.** Peuravuori and Pihlaja (2004) **21.** Mayo et al. (2004) **22.** Chalmers and Griffiths (2002) **23.** Ascough et al. (2011) **24.** Stevenson (1994) **25.** Hay and Myneni (2007) **26.** Ilani et al. (2005) **27.** Pike et al. (1993)

The FTIR spectra of the CLY sample showed notable differences in the location and intensities of peaks in comparison to the peaks observed in RBS, SLT, and AQS (Fig. 2b). The absorbance band attributed to various O—H stretching in the CLY spectra was centered at 3360 cm^{-1} and contained an additional peak at 3230 cm^{-1}, which may indicate a higher occurrence of the H-bonded O—H stretching of carboxylic acid and increased contributions from the N–H stretch of amide II, respectively. Furthermore, a broad shoulder between 3100 and 3030 cm^{-1}, which is attributed to aromatic C–H stretching, showed higher relative absorbance compared to the other samples, whereas the aliphatic C–H stretch between 2970 and 2820 cm^{-1} was less pronounced in the CLY spectrum compared to the other samples. In the 1800 and 1500 cm^{-1} range, the CLY spectrum was similar to the spectra of the other samples, however, CLY contained a dominant peak at 1395 cm^{-1}. The downward shift of this peak to slightly lower wavenumbers than that of the other sample spectra (~1440 cm^{-1}) indicates lower absorbance from aliphatic C–H deformation and drastically higher absorbance from C—O stretching of carboxylic derivatives (i.e., sodium benzoate) and asymmetric COO$^-$ stretching. In comparison to the other samples, CLY shows only minor absorbance between ~1180 and 1000 cm^{-1} and a relatively small peak at 880 cm^{-1} corresponding to C–O–C and C-O-H stretches of polysaccharide moieties and an out-of-plane bending of aromatic CH, respectively.

3.2 *Distribution of functional groups in sedimentary organic matter*

The relative contribution of each of the assigned functional groups to the overall sample SOM were estimated by taking the area under the peak between the wave numbers assigned to each functional group (Table 2). The major functional groups contributing to the SOM observed in the samples were aromatic rings (C–H at 3100-3030 and 900-860 cm^{-1}; C=C stretch at 1630-1600, 1570-1550, and 1515-1490 cm^{-1}), aliphatic C–H (2970-2820 and 1470-1430 cm^{-1}), carbonyl (1670-1630 cm^{-1}), protonated carboxyl groups (1720-1690 cm^{-1}), deprotonated carboxyl groups attached to an aromatic ring (aromatic carboxylate groups, 1420-1370 cm^{-1}), and carbohydrate (1180-1000 cm^{-1}) (Fig. 3). Results show that the RBS, SLT, and AQS had similar aromatic to aliphatic (Ar:Al) ratios (0.66, 0.60, 0.89, respectively), whereas CLY had a much higher Ar:Al (1.86) (Fig. 3). The primary reason for a markedly high Ar:Al in CLY is the large contribution of aromatic carboxylate structures (1420-1370 cm^{-1}) in the spectrum (36%), which increased with depth from the overlying RBS, SLT, and AQS samples (12%, 13%, and 19%, respectively) (Table S2).

One effect of alkali extractions is the deprotonation of dissociable carboxylic acid groups, which diminish the COOH absorbance bands in the FTIR spectra between 1720-1700 cm^{-1}, and increase absorbance between 1400-1370 cm $^{-1}$ (Hay & Myneni, 2007; Nuzzo et al., 2020). These bands are commonly attributed to the carboxyl groups of sodium benzoate, which increase along with rising pH (Hayes et al., 1989; Guan et al., 2006; Lee & Seo, 2014). A comparison of the peaks at ~1720 and ~1400 cm^{-1} suggests that most of the carboxyl groups in the SOM of all samples were deprotonated. The accumulation of simple compounds such as benzene and carboxylate derivatives with greater depth infer a higher level of humification, indicating that CLY contains much higher relative proportions of a more degraded (i.e., humified) pool of SOM (Table S3).

The contributions from aliphatic C– H were found to be higher in RBS (37%) and AQS (37%) than in the finer grain SLT (32%) and CLY (24%) samples. However, neither grain size nor depth could solely explain the distribution of functional groups in the SOM as SLT contained a relatively large amount of carbohydrates (17%) while only trace amounts were present in CLY (<1%). Relative proportions of carbohydrates in the RBS and AQS were 9% and 5%, respectively. The proportions of the peaks assigned strictly to aromatic rings were comparable among RBS, SLT, AQS and CLY (28%, 25%, 28% and 29%, respectively), whereas carbonyl groups were found in slightly higher proportions in the RBS, SLT, and AQS (9%, 9%, 7%, respectively), than CLY (6%).

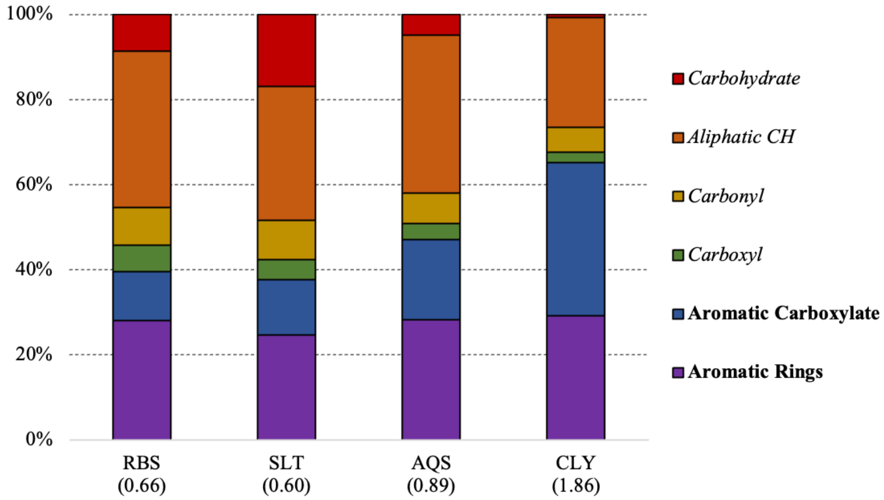

Figure 3. Proportions of functional groups in the sediment samples. **Bold** font represents groups attributed to aromatic structures and *Italicized* font represents groups attributed to aliphatic structures (Li et al., 2015). Value in parenthesis is the Ar:Al for each sample. The riverbank sand, silt, aquifer sand, and the clay aquitard are denoted by RBS, SLT, AQS, and CLY, respectively.

336

Table 2. Area under the peak for the assigned functional groups in the FTIR spectra. The riverbank sand, silt, aquifer sand, and the clay aquitard are denoted by RBS, SLT, AQS, and CLY, respectively.

Sample	Aliphatic CH	Carboxyl	Carbonyl	Aromatic Ring	Aromatic-Carboxylate	Carbohydrate	Total Area	Aromatic: Aliphatic
RBS	10.92	1.80	2.62	8.31	3.41	2.55	29.60	0.66
SLT	15.43	2.25	4.48	11.97	6.41	8.23	48.77	0.60
AQS	22.31	2.23	4.34	16.95	11.46	2.98	60.28	0.89
CLY	23.79	2.38	5.28	26.72	33.01	0.59	91.78	1.86
Aldrich HA	10.34	11.43	3.38	37.07	-	11.29	73.51	1.26

3.3 Fluorescence characteristics of SOM

The absorbance and fluorescence of the aqueous NaOH extracts provide a more robust characterization of the SOM properties which may impact geochemical processes in the riverbank and aquifer (Fig. 4). The SOM in the RBS, SLT, AQS, and CLY is from a terrestrial source (FI = 1.35, 1.32, 1.44, and 1.27, respectively). The age of the SOM is reflected by the freshness index which shows that the SOM within RBS and SLT (β:α = 0.73 and 0.82, respectively) is more recently produced relative to the more degraded SOM found in the AQS and CLY (β:α = 0.53 and 0.63, respectively) (Table S3) which concurs with the depositional history. The presence of aromatic structures, as indicated by the absorbance at 254 nm (abs254), were elevated in the CLY (11.07) relative to the RBS, SLT, and AQS (1.33, 1.52, and 0.79, respectively).

Four primary peaks were identified in the excitation and emission spectra of the samples for the peak-picking method (Table S3, Fig. 4), including; peak A (terrestrial humic-like), peak T (protein-like), peak C (terrestrial fulvic-like), and peak M (microbially produced, humic-like) (Coble et al., 1998). The peak typically attributed to tyrosine protein-like fluorescence (peak B) was not present in any of the samples. In general, the fluorescence indices show that the sample SOM is composed largely of humic and fulvic-like compounds (60-70%) with varying proportions of protein-like (1-7%) and microbially produced compounds (29-35%). The proportions represented by each peak were similar among each the samples, ranging between 43-48%, 17-19%, 29-35%, and 1-7% for peaks A, C, M, and T, respectively. However, the highest proportions of protein-like and microbially produced SOM are observed in the SLT as shown by a lower humic:protein ratio (humic:protein = 6.1) and higher microbial: terrestrial ratio (peak M/peak C = 2.0) compared to the RBS (9.2 and 1.68), AQS (24.0 and 1.83), and CLY (9.0 and 1.45) (Table S3).

The absorbance and fluorescence data complemented the FTIR results and provided further characterization of the variations in the SOM in the riverbank and aquifer sediments. Variations in SOM reactivity can be visualized by comparing the humic and fulvic-like signatures (peak A and C) with the protein-like and microbially produced SOM (peaks T and M) as it relates to the distribution of functional groups. For example, the sum of peaks T and M were positively correlated with the proportions of carbohydrate ($R^2 = 0.91$) and carbonyl ($R^2 = 0.71$) in the SOM, whereas the sum of peaks A and C are positively correlated with aromatic structures ($R^2 = 0.73$). Furthermore, the Ar:Al obtained from the assignment of the functional groups showed a positive association with both the humification index (HIX, $r = 0.78$) and abs254 ($r = 0.96$), which in turn were each negatively correlated with the proportions of aliphatic CH ($r = -1.00$ and -0.90, respectively) and positively correlated with the proportions of aromatic carboxylate ($r = 0.77$ and 0.94, respectively) (Fig. S2). Fulvic-like SOM showed positive correlation with aromatic rings (peak C, $r = 0.98$) whereas humic-like SOM was more closely associated with the aromatic-carboxyl structures (peak A, $r = 0.90$). The relative proportions of humic-like SOM were negatively correlated with those of carbonyl and carbohydrates ($r = -0.87$, and -0.88, respectively). Conversely, the proportions of carbonyl and carbohydrate functional groups in the SOM were positively correlated with $\beta:\alpha$ ($r = 0.72$ and 0.80, respectively) and the M:C ratio ($r = 0.73$ and 0.83, respectively). However, the relative proportions of carbonyl functional groups were more closely related to microbially produced SOM (peak M, $r = 0.57$) whereas the proportion of carbohydrates were associated with the proportions of protein-like SOM ($r = 0.68$). Whereas these correlations provide valuable insights between optical properties and functional group distributions, their statistical significance shall be interpreted with caution because of the limited number of samples analyzed in this study. Although the potential heterogeneity in the individual sample type was not addressed in this study, the functional group distribution among four types of samples (RBS, SLT, AQS and CLY) is clearly distinguishable.

The PARAFAC model validated three components (Fig. S3) utilizing the 96 sample dataset comprised of samples from this study (n = 4) and samples from previous work (Varner et al., 2022) along the Meghna riverbank (92). The samples included in the PARAFAC model from this study were the NaOH sediment-extracts and differed from the remaining 92 samples, which were all measured for UV-Vis properties in a water-based medium. Despite showing a similar proportion of components, the samples from this study contained much higher overall values for the components, specifically for component 1 (Table S1). Due to the lack of representation of similar sample types in the 96 sample PARAFAC model, we determined that the model is not the best representation of the OM characteristics for these samples. However, the components included in the model remain consistent regardless of sample type, therefore, we have included the model results in the supplementary information.

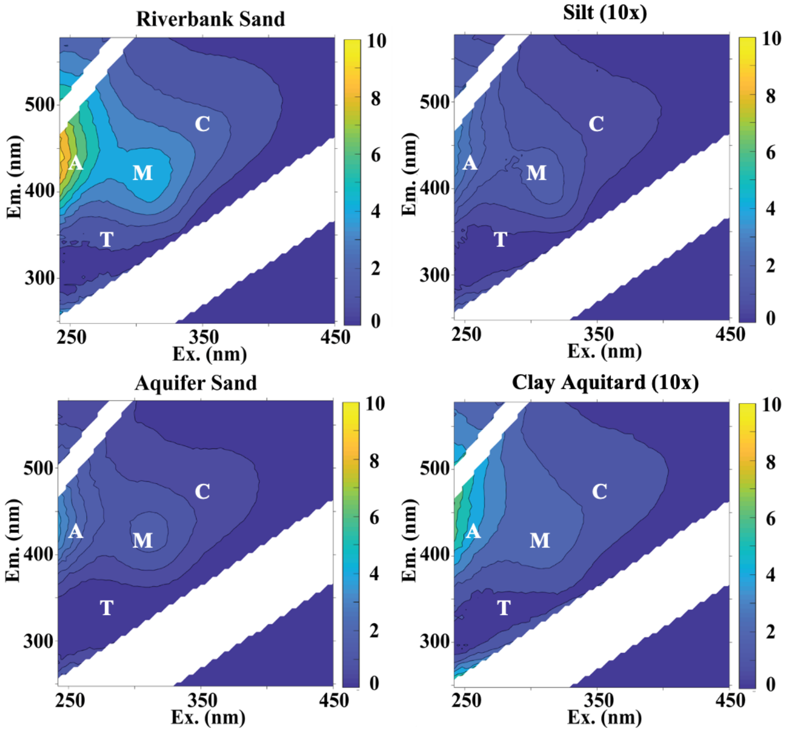

Figure 4. Excitation emission matrices of the samples. The silt and clay aquitard EEMs displayed are 10x diluted. All intensities are reported in Raman Unit (R.U.) 396

4 Discussion

4.1 *Properties of SOM in the Aquifer and Riverbank sediments*

The complimentary techniques used to characterize the spectroscopic properties of SOM revealed variations its properties among the riverbank and aquifer sediments. In general, the relationship between the humification index (HIX) with the proportions of aromatic rings, aliphatic CH, and aromatic-carboxyl structures suggests that these functional groups are indicative of more humified SOM. Conversely, younger, and supposedly more reactive SOM typically contains higher proportions of both carbonyl (Amide I) and carbohydrates which are associated with protein-like and microbially produced SOM. Interestingly, none of the identified SOM properties are reliably correlated to sediment grain size. For example, the SLT and CLY, apart from demonstrating a similar terrestrial source and higher HIX than the sand samples, varied in their chemical composition. The SOM in the CLY was characterized by more highly degraded aromatic and carboxyl compounds of humic-acids and contained minimal proportions of labile OM such as carbohydrate (1%) and carbonyl groups (6%) (Fig. 3). The SOM in the SLT, on the other hand, showed higher proportions of protein-like and microbially produced SOM and was relatively enriched in carbohydrates (17%) and carbonyl (9%). Freshly produced substances, such as carbohydrates, have a large impact on the interactions between SOM and its surroundings since carbohydrates are highly labile and preferentially utilized for microbial degradation as opposed to more humified material (Wu et al., 2009; Gustafsson et al., 2014; Shi et al., 2016; Lu et al., 2017). The properties of SOM in the coarse grained RBS and AQS were similar, although the composition of the SOM in RBS more closely resembled that of the near surface SLT SOM with slightly higher proportions of more labile carbonyl and carbohydrates (9% and 9% respectively) relative to AQS (7% and 5%, respectively).

Aromatic compounds have been shown to contain highly adsorbing properties (Coward et al., 2018; Groeneveld et al., 2020), yet in this study, the SOM from the samples of various lithologies contain similar proportions of aromatic rings (25-29%). Further resolution is provided by the assignment of the peak at ~1400 cm^{-1} to aromatic carboxylate groups, which form under alkaline conditions. Evidence for the assignment of this peak to aromatic carboxylate groups and is further supported by the relationship between the Ar:Al and both the HIX ($r = 0.78$) and abs254 ($r = 0.96$), which indicate the degree of humification and aromaticity, respectively (Fig. S2) (Ohno, 2002; Weishaar et al., 2003; Zsolnay, 2003). While a similar proportion of aromatic rings were observed in RBS, SLT, AQS, and CLY (28%, 25%, 28%, 29%, respectively), the RBS, SLT, and AQS contained higher proportions of aliphatic C–H than CLY (37%, 32%, 37%, 26%, respectively). Owing to the diverse properties of natural SOM, the predominance of neither aliphatic nor aromatic compounds in the SOM can be used exclusively to explain the sorption affinity of SOM (Chefetz & Xing, 2009). Nevertheless, a substantial pool of SOM is comprised of both aromatic compounds with a high sorption affinity (Weber Jr et al., 1992; Chin et al., 1997; Tremblay et al., 2005; Tang & Weber, 2006), and aliphatic components which serve as a prominent sorption material for both organic matter (Chefetz et al., 2000; Chefetz, 2003; Lin et al., 2007; Sun et al., 2008) and iron minerals (Adhikari & Yang, 2015). Adhikari and Yang (2015) found that aliphatic carbon may bind to Fe-oxides and remain adsorbed even if the Fe-oxides become reduced, allowing for the accumulation of aliphatic carbon in older pools of SOM. The area under the peaks associated with both aliphatic C–H and aromatic rings increases with the sample depth (RBS < SLT < AQS < CLY) (Table S1). As humification proceeds over time, the degradation of more characteristic structures results in the enhancement of refractory signals from simpler aromatic and aliphatic compounds (Kelleher et al., 2006; Chefetz & Xing, 2009). This finding of increasing abundance of humified SOM structures with depth (Fig. 3) is consistent with the accumulation of humic-like, aromatic SOM in the shallow aquifer sediments of Bangladesh under reducing conditions (McArthur et al., 2004; Mladenov et al., 2010; Datta et al., 2011).

4.2 Varying influence of SOM on As and Fe mobility

As presented above, a notable finding from the distribution of the functional groups in the SOM is the observed differences between the fine grain samples SLT and CLY. Whereas previous studies demonstrate the correlation between the concentrations of SOM, As, and Fe in the reducing shallow aquifers of Bangladesh (Dowling et al., 2002; Harvey et al., 2002; Anawar et al., 2003; Stüben et al., 2003), the extent that fine grain layers within the shallow aquifer play in promoting As mobility remains uncertain. Regardless, it is widely agreed that OM drives the redox reactions governing the microbially mediated release of As (Bauer & Blodau, 2006; Cui & Jing, 2019), yet some fractions of SOM may regulate As mobility through differing mechanisms depending on the specific chemical properties (Anawar et al., 2013). For example, OM may strongly adsorb onto the surface of positively charged Fe-minerals (Sharma et al., 2010; Mladenov et al., 2015), which may regulate As mobility by displacing any adsorbed As (Bauer & Blodau, 2009), or forming ternary As-Fe-OM complexes via cationic bridging (Redman et al., 2002; Liu et al., 2011; Mikutta & Kretzschmar, 2011; de Oliveira et al., 2015; Liu et al., 2020b; Aftabtalab et al., 2022). Therefore, the behavior of sedimentary and dissolved As are linked to the interactions between various OM functional groups and Fe.

Furthermore, the peak at ~1400 cm^{-1} in the FTIR spectra is also often attributed to ligand exchange mechanisms associated with carboxylate-Fe bonds (Gu et al., 1994; Fu & Quan, 2006; Kaiser & Guggenberger, 2007; Oren & Chefetz, 2012; Liu et al., 2020a). Carboxyl groups are important mediators in the SOM fraction of soils, capable of promoting ion exchange reactions to extract metal cations from the sediment and groundwater (Wu et al., 2009; Gustafsson et al., 2014; Shi et al., 2016; Lu et al., 2017). This tendency allows for carboxylate groups to be highly effective at sequestering Fe-minerals (Curti et al., 2021; Wen et al., 2022). However, most carboxylic acid derivatives are water soluble throughout the pH ranges found in natural groundwater (Fox et al., 2017), and have been implicated in the co-occurrence of DOC and Fe in the porewaters of sediments containing carboxyl-rich SOM (Curti et al., 2021; Liu et al., 2022). In the case of the Meghna riverbank and aquifer sediments, the proportions of aromatic carboxylate groups in the SOM show positive correlation to depth and also to the water extractable concentrations of As and Fe previously measured on the same sediment samples (Varner et al., 2022) (Fig. S4). The abundance of aromatic carboxylate groups in the CLY sample suggests that the SOM here may maintain elevated As concentrations in the groundwater by providing an ample source of carboxyl-rich OM to the aquifer that favors the formation of soluble As-Fe-OM complexes. This idea is consistent with previous findings suggesting that clay layers in the shallow aquifers of Bangladesh are a prominent source of the DOC that sustains As mobility (Mukherjee et al., 2007a; Mukherjee et al., 2007b; Guo et al., 2019; Mihajlov et al., 2020).

The SOM in the SLT contains relatively high proportions of polysaccharides (17%), which have the potential to be utilized as electron donors for heterotrophic microbial respiration under both aerobic and anoxic conditions (Zhang et al., 2019) and are often indicative of high levels of microbial activity (Laspidou & Rittmann, 2002; Omoike et al., 2004). In nature, the role of microbial activity is ubiquitous and polysaccharides present a major labile energy source for bacteria, so that under reducing conditions, polysaccharides support the heterotrophic metabolisms driving the microbially mediated reduction of the OM-bearing Fe-oxides (Haider, 2021). Similarly, the RBS, SLT, and AQS contain higher proportions of carbonyl groups assigned to the peak at ~1650 cm^{-1} (8.9%, 9.2%, 7.2%, respectively) than the CLY (5.8%). This peak is typically attributed to the C=O stretch of carbonyl bonded to proteinaceous amine (amide I). The SOM in the SLT contained the highest proportions of carbonyl and also contained the highest β:α values and proportions of peak T, indicating the presence of freshly produced proteinaceous material (Fig. 3, Table S3). In general, the higher proportions of carbonyl components in the RBS, SLT, and AQS support the biological activity that may promote the microbial reduction of As-bearing Fe-oxide minerals (McArthur et al., 2001; Glodowska et al., 2020; Qiao et al., 2020).

Overall, the reactivity of SOM as it relates to As and Fe in the sediment can be summarized by the Ar:Al and the HIX (Fig. S4). The SOM with higher HIX is associated with elevated sedimentary As and water-extractable As concentrations. In contrast, water-extractable Fe concentrations are more closely related to the Ar:Al than the HIX (Fig. S4). These findings are consistent with previous work which showed that humic-like OM is linked to elevated As content within the groundwaters of the Bengal basin (Vega et al., 2017; Kulkarni et al., 2018a) and that Fe preferentially co-precipitates with more aromatic OM (Du et al., 2018). Elevated proportions of carbohydrate and carbonyl along with lower proportions of aliphatic CH and carboxyl groups indicate a fresher and more labile source of carbon in the near-surface SLT sediment, whereas the deeper CLY sediment is rich in carboxylic derivatives favoring the formation of soluble OM-Fe-As complexes. Comparing the SOM properties between SLT and CLY suggests that not all fine grain layers in the shallow aquifers of Bangladesh contribute to As mobilization similarly.

4.3 Potential impacts of SOM on As mobility in hyporheic zone sediments

The extent of As enrichment in the Meghna River HZ has previously been shown to be influenced by the grain size of the surficial sediments wherein sandy sediments promote the surface water-groundwater mixing required for the precipitation of As-attenuating Fe-oxides, and a surficial silt layer prohibits the mixing and prevents the accumulation of sedimentary As (Jung et al., 2015). Furthermore, the presence of fine grain sediments along the Red River in Vietnam have been implicated in the propagation of a high As plume in the adjacent aquifer by contributing to the persistent reduction of reactive Fe-oxides within the riverbank sediments (Stahl et al., 2016; Wallis et al., 2020). The influence of a shallow buried silt layers (3-7 m bgl) underlying riverbank sands have not been studied in relation to the occurrence of As enrichment in HZ sediments, although we hypothesize that the silt layer may limit surface water-groundwater mixing and also provide a source of labile SOM to drive reductive processes. This may explain the markedly lower sedimentary As concentrations in the HZ at this site (7 ± 2 mg/kg) (Varner et al., 2022) compared to other measurements within the Meghna River HZ which commonly exceeded 500 mg/kg (Datta et al., 2009; Jung et al., 2015; Berube et al., 2018). Together, the SOM properties of the HZ sediments (SLT and RBS) indicate young, labile SOM with higher electron donating capacities than the underlying aquifer sediments. This is shown by the high proportions of both carbohydrates (16.9%) and carbonyl groups (9.2%) in the SLT samples, which are elevated compared to both the RBS (8.6% and 8.9%, respectively) and to the underlying AQS (4.9% and 7.2%, respectively). In this case, the silt layer can serve as a source of labile OM to the overlying HZ which promotes reducing conditions, preventing the accumulation of Fe-oxides which are capable of attenuating As in the HZ sediment.

In contrast, the SOM in the CLY contains a more humified and recalcitrant pool of carboxyl-rich SOM with a tendency to form soluble As and Fe complexes. These soluble complexes may contribute to elevated dissolved As concentrations in the aquifer should they be mobilized. Sands comprising the shallow aquifers (<60 m) in the Bengal Basin host the highest concentrations of dissolved As and Fe (Nickson et al., 1998; Harvey et al., 2002; Huq et al., 2020), which are often maintained in solution through complexation with more soluble portions of humic-like DOC (Sharma et al., 2010; Liu et al., 2011; Wu et al., 2019). Therefore, varying reactivity and nature of the SOM in the HZ sediments, shallow buried silt, and the underlying aquifer sediments may affect As mobility through differing mechanisms. The detailed characterization of the SOM at this site indicates the varying roles that SOM has on regulating As mobility in the HZ. Regardless, the extent that SOM impacts As mobility within the HZ is largely influenced by the groundwater flow patterns and thus further research into the temporal and spatial flow patterns along the Meghna River is warranted.

5 Conclusion

This study characterized the chemical reactivity of SOM from the HZ sediments along the Meghna River, Bangladesh and an As contaminated aquifer adjacent to the river. The SOM in both the riverbank and aquifer sands was shown to have a similar terrestrial source containing both humic-like and fulvic-like signatures. Variations in the chemical composition of the SOM in the shallow silt and clay aquitard revealed a more recalcitrant and degraded SOM in the underlying clay aquitard with a high aromatic carboxylate content whereas the aquifer silt at ~3 m bgl contained fresher, microbially produced SOM with higher proportions of amides and polysaccharide moieties. The carboxylate-rich clay aquitard may support As mobility by favoring the formation of soluble Fe and As complexes, while the labile SOM in the aquifer silt may promote As mobilization by fueling the microbially mediated dissolution of As-bearing Fe-oxides.

Within the HZ, the SOM and groundwater flow controls of the shallow buried silt layer may act together inhibit the accumulation of sedimentary As. Higher proportions of labile OM in the aquifer silt and riverbank sands support the microbially-mediated reductive dissolution of As-bearing Fe-oxides under reducing conditions, preventing the accumulation of sedimentary As.

Should the reactive SOM in the silt layer contribute to the dissolved load of the discharging groundwater during the dry season, the production of Fe-oxides may be limited by the influx of reactive DOC. These findings suggest that the variable SOM characteristics along the Meghna River and its adjacent aquifer contain differing reactive properties that regulate the geochemical processes governing As and Fe mobility. This study contributes to our understanding of the contrasting roles that SOM may have on As mobility within both riverine aquifers and the HZ along the river water-groundwater interface.

6 Acknowledgements

We thank the students at the University of Dhaka for assistance in the field. We would like to thank Dr. Audrey Lamb's lab group at UTSA for assisting with the lyophilization process and the UTSA Chemistry Department for providing access to the FTIR instrument. Funding was provided to Peter S. Knappett, M. Bayani Cardenas, and Saugata Datta by the National Science Foundation Hydrologic Sciences grant numbers EAR- 1852652, EAR- 1852653, and EAR- 1940772, respectively.

Commented [CMB1]: Please name them all. Else, this is pretty hollow and might have the counter effect of being offensive/irritating.

7 Credit author statement

Thomas Varner: Conceptualization, Methodology, Validation, Formal analysis, Investigation, Data curation, Writing original draft, Visualization. Harshad V. Kulkarni: Conceptualization, Methodology, Validation, Formal analysis, Investigation, Data curation, Writing – review & editing, Visualization, Supervision. Peter Knappett: Resources, Writing – review and editing, Project administration, Funding acquisition. Bayani Cardenas: Resources, Writing – review and editing, Project administration, Funding acquisition. Saugata Datta: Conceptualization, Resources, Writing – review and editing, Project administration, Supervision, Funding acquisition.

8 References

Adhikari, D., & Yang, Y. (2015). Selective stabilization of aliphatic organic carbon by iron oxide. *Scientific reports*, *5*(1), 1-7.

Aeschbacher, M., Sander, M., & Schwarzenbach, R. P. (2010). Novel electrochemical approach to assess the redox properties of humic substances. *Environmental Science & Technology*, *44*(1), 87-93.

Aftabtalab, A., Rinklebe, J., Shaheen, S. M., Niazi, N. K., Moreno-Jiménez, E., Schaller, J., & Knorr, K.-H. (2022). Review on the interactions of arsenic, iron (oxy)(hydr) oxides, and dissolved organic matter in soils, sediments, and groundwater in a ternary system. *Chemosphere*, *286*, 131790.

Anawar, H. M., Akai, J., Komaki, K., Terao, H., Yoshioka, T., Ishizuka, T., Safiullah, S., & Kato, K. (2003). Geochemical occurrence of arsenic in groundwater of Bangladesh: sources and mobilization processes. *Journal of Geochemical Exploration*, *77*(2-3), 109-131.

Anawar, H. M., Tareq, S. M., & Ahmed, G. (2013). Is organic matter a source or redox driver or both for arsenic release in groundwater? *Physics and Chemistry of the Earth, Parts A/B/C*, *58*, 49-56.

Appelo, C., Van der Weiden, M., Tournassat, C., & Charlet, L. (2002). Surface complexation of ferrous iron and carbonate on ferrihydrite and the mobilization of arsenic. *Environmental Science & Technology*, *36*(14), 3096-3103.

Ascough, P. L., Bird, M. I., Francis, S., & Lebl, T. (2011). Alkali extraction of archaeological and geological charcoal: evidence for diagenetic degradation and formation of humic acids. *Journal of Archaeological Science*, *38*(1), 69-78.

Aziz, Z., van Geen, A., Stute, M., Versteeg, R., Horneman, A., Zheng, Y., Goodbred, S., Steckler, M., Weinman, B., Gavrieli, I., Hoque, M. A., Shamsudduha, M., & Ahmed, K. M. (2008). Impact of local recharge on arsenic concentrations in shallow aquifers inferred from the electromagnetic conductivity of soils in Araihazar, Bangladesh. *Water Resources Research*, *44*(7). https://doi.org/10.1029/2007wr006000

Bai, Y., Subdiaga, E., Haderlein, S. B., Knicker, H., & Kappler, A. (2020). High-pH and anoxic conditions during soil organic matter extraction increases its electron-exchange capacity and ability to stimulate microbial Fe (III) reduction by electron shuttling. *Biogeosciences*, *17*(3), 683-698.

Baken, S., Salaets, P., Desmet, N., Seuntjens, P., Vanlierde, E., & Smolders, E. (2015). Oxidation of iron causes removal of phosphorus and arsenic from streamwater in groundwater-fed lowland catchments. *Environmental Science & Technology*, *49*(5), 2886-2894.

Bauer, M., & Blodau, C. (2006). Mobilization of arsenic by dissolved organic matter from iron oxides, soils and sediments. *Science of The Total Environment*, *354*(2-3), 179-190.

Bauer, M., & Blodau, C. (2009). Arsenic distribution in the dissolved, colloidal and particulate size fraction of experimental solutions rich in dissolved organic matter and ferric iron. *Geochimica et Cosmochimica Acta*, *73*(3), 529-542.

Bellamy, L. (2013). *The infra-red spectra of complex molecules*.Springer Science & Business Media.

Berube, M., Jewell, K., Myers, K. D., Knappett, P. S., Shuai, P., Hossain, A., Lipsi, M., Hossain, S., Aitkenhead-Peterson, J., & Ahmed, K. (2018). The fate of arsenic in groundwater discharged to the Meghna River, Bangladesh. *Environ. Chem.*, *15*, 29.

BGS&DPHE. (2001). *Arsenic contamination of groundwater in Bangladesh*.

Bhattacharya, P., Jacks, G., Jana, J., Sracek, A., Gustafsson, J., & Chatterjee, D. (2001). Geochemistry of the Holocene alluvial sediments of Bengal Delta Plain from West Bengal, India: implications on arsenic contamination in groundwater. *Groundwater arsenic contamination in the Bengal Delta Plain of Bangladesh*, *3084*, 21-40.

Bibi, M. H., Ahmed, F., & Ishiga, H. (2008). Geochemical study of arsenic concentrations in groundwater of the Meghna River Delta, Bangladesh. *Journal of Geochemical Exploration*, *97*(2-3), 43-58.

Biswas, A., Majumder, S., Neidhardt, H., Halder, D., Bhowmick, S., Mukherjee-Goswami, A., Kundu, A., Saha, D., Berner, Z., & Chatterjee, D. (2011). Groundwater chemistry and redox processes: depth dependent arsenic release mechanism. *Applied geochemistry*, *26*(4), 516-525.

Bone, S. E., Gonneea, M. E., & Charette, M. A. (2006). Geochemical cycling of arsenic in a coastal aquifer. *Environmental Science & Technology*, *40*(10), 3273-3278.

Borisover, M., Lordian, A., & Levy, G. J. (2012). Water-extractable soil organic matter characterization by chromophoric indicators: Effects of soil type and irrigation water quality. *Geoderma*, *179*, 28-37.

Bustin, R., & Guo, Y. (1999). Abrupt changes (jumps) in reflectance values and chemical compositions of artificial charcoals and inertinite in coals. *International Journal of Coal Geology*, *38*(3-4), 237-260.

Chalmers, J. M., & Griffiths, P. R. (2002). *Handbook of vibrational spectroscopy* (Vol. 4). Wiley.

Charette, M. A., & Sholkovitz, E. R. (2002). Oxidative precipitation of groundwater-derived ferrous iron in the subterranean estuary of a coastal bay. *Geophysical Research Letters*, *29*(10), 85-81-85-84.

Charette, M. A., & Sholkovitz, E. R. (2006). Trace element cycling in a subterranean estuary: Part 2. Geochemistry of the pore water. *Geochimica et Cosmochimica Acta*, *70*(4), 811-826.

Charette, M. A., Sholkovitz, E. R., & Hansel, C. M. (2005). Trace element cycling in a subterranean estuary: Part 1. Geochemistry of the permeable sediments. *Geochimica et Cosmochimica Acta*, *69*(8), 2095-2109.

Chefetz, B. (2003). Sorption of phenanthrene and atrazine by plant cuticular fractions. *Environmental Toxicology and Chemistry: An International Journal*, *22*(10), 2492-2498.

Chefetz, B., Deshmukh, A. P., Hatcher, P. G., & Guthrie, E. A. (2000). Pyrene sorption by natural organic matter. *Environmental Science & Technology*, *34*(14), 2925-2930.

Chefetz, B., Hader, Y., & Chen, Y. (1998). Dissolved organic carbon fractions formed during composting of municipal solid waste: properties and significance. *Acta hydrochimica et hydrobiologica*, *26*(3), 172-179.

Chefetz, B., & Xing, B. (2009). Relative role of aliphatic and aromatic moieties as sorption domains for organic compounds: a review. *Environmental Science & Technology*, *43*(6), 1680-1688.

Chen, W., & Yu, H.-Q. (2021). Advances in the characterization and monitoring of natural organic matter using spectroscopic approaches. *water research*, *190*, 116759.

Chin, Y.-P., Aiken, G. R., & Danielsen, K. M. (1997). Binding of pyrene to aquatic and commercial humic substances: the role of molecular weight and aromaticity. *Environmental Science & Technology*, *31*(6), 1630-1635.

Coble, P. G., Del Castillo, C. E., & Avril, B. (1998). Distribution and optical properties of CDOM in the Arabian Sea during the 1995 Southwest Monsoon. *Deep Sea Research Part II: Topical Studies in Oceanography*, *45*(10-11), 2195-2223.

Coble, P. G., Lead, J., Baker, A., Reynolds, D. M., & Spencer, R. G. (2014). *Aquatic organic matter fluorescence*.Cambridge University Press.

Coble, P. G., & Timperman, A. T. (1998). Fluorescence detection of proteins and amino acids in capillary electrophoresis using a post-column sheath flow reactor. *Journal of Chromatography A*, *829*(1-2), 309-315.

Coward, E. K., Ohno, T., & Sparks, D. L. (2018). Direct evidence for temporal molecular fractionation of dissolved organic matter at the iron oxyhydroxide interface. *Environmental Science & Technology*, *53*(2), 642-650.

Cui, J., & Jing, C. (2019). A review of arsenic interfacial geochemistry in groundwater and the role of organic matter. *Ecotoxicology and Environmental Safety*, *183*, 109550.

Curti, L., Moore, O. W., Babakhani, P., Xiao, K.-Q., Woulds, C., Bray, A. W., Fisher, B. J., Kazemian, M., Kaulich, B., & Peacock, C. L. (2021). Carboxyl-richness controls organic carbon preservation during coprecipitation with iron (oxyhydr) oxides in the natural environment. *Communications Earth & Environment*, *2*(1), 1-13.

Datta, S., Mailloux, B., Jung, H.-B., Hoque, M., Stute, M., Ahmed, K., & Zheng, Y. (2009). Redox trapping of arsenic during groundwater discharge in sediments from the Meghna riverbank in Bangladesh. *Proceedings of the National Academy of Sciences*, *106*(40), 16930-16935.

Datta, S., Neal, A. W., Mohajerin, T. J., Ocheltree, T., Rosenheim, B. E., White, C. D., & Johannesson, K. H. (2011). Perennial ponds are not an important source of water or dissolved organic matter to groundwaters with high arsenic concentrations in West Bengal, India. *Geophysical Research Letters*, *38*(20).

de Melo Benites, V., de Sá Mendonça, E., Schaefer, C. E. G., Novotny, E. H., Reis, E. L., & Ker, J. C. (2005). Properties of black soil humic acids from high altitude rocky complexes in Brazil. *Geoderma*, *127*(1-2), 104-113.

de Oliveira, L. K., Melo, C. A., Goveia, D., Lobo, F. A., Armienta Hernández, M. A., Fraceto, L. F., & Rosa, A. H. (2015). Adsorption/desorption of arsenic by tropical peat: influence of organic matter, iron and aluminium. *Environmental Technology*, *36*(2), 149-159.

Deng, Y., & Dixon, J. B. (2002). Soil organic matter and organic-mineral interactions. *Soil mineralogy with environmental applications*, *7*, 69-107.

Dowling, C. B., Poreda, R. J., Basu, A. R., Peters, S. L., & Aggarwal, P. K. (2002). Geochemical study of arsenic release mechanisms in the Bengal Basin groundwater. *Water Resources Research*, *38*(9), 12-11-12-18.

Du, Y., Ramirez, C. E., & Jaffé, R. (2018). Fractionation of dissolved organic matter by co-precipitation with iron: effects of composition. *Environmental Processes*, *5*(1), 5-21.

Fernández-Getino, A., Hernández, Z., Buena, A. P., & Almendros, G. (2010). Assessment of the effects of environmental factors on humification processes by derivative infrared spectroscopy and discriminant analysis. *Geoderma*, *158*(3-4), 225-232.

Fiebig, D. M. (1995). Groundwater discharge and its contribution of dissolved organic carbon to an upland stream. *Archiv für Hydrobiologie*, *134*(2), 129-155.

Findlay, S., Sinsabaugh, R. L., Sobczak, W. V., & Hoostal, M. (2003). Metabolic and structural response of hyporheic microbial communities to variations in supply of dissolved organic matter. *Limnology and Oceanography*, *48*(4), 1608-1617.

Fischer, H., Kloep, F., Wilzcek, S., & Pusch, M. T. (2005). A river's liver–microbial processes within the hyporheic zone of a large lowland river. *Biogeochemistry*, *76*(2), 349-371.

Flanagan, S. V., Johnston, R. B., & Zheng, Y. (2012). Arsenic in tube well water in Bangladesh: health and economic impacts and implications for arsenic mitigation. *Bulletin of the World Health Organization*, *90*, 839-846.

Fox, P. M., Nico, P. S., Tfaily, M. M., Heckman, K., & Davis, J. A. (2017). Characterization of natural organic matter in low-carbon sediments: Extraction and analytical approaches. *Organic Geochemistry*, *114*, 12-22.

Fu, H., & Quan, X. (2006). Complexes of fulvic acid on the surface of hematite, goethite, and akaganeite: FTIR observation. *Chemosphere*, *63*(3), 403-410.

Fultz, L. M., Moore-Kucera, J., Calderón, F., & Acosta-Martínez, V. (2014). Using Fourier-Transform Mid-Infrared Spectroscopy to Distinguish Soil Organic Matter Composition Dynamics in Aggregate Fractions of Two Agroecosystems. *Soil Science Society of America Journal*, *78*(6), 1940-1948.

Glodowska, M., Stopelli, E., Schneider, M., Lightfoot, A., Rathi, B., Straub, D., Patzner, M., Duyen, V., Members, A. T., & Berg, M. (2020). Role of in situ natural organic matter in mobilizing As during microbial reduction of FeIII-mineral-bearing aquifer sediments from Hanoi (Vietnam). *Environmental Science & Technology*, *54*(7), 4149-4159.

Goldman, J. H., Rounds, S. A., & Needoba, J. A. (2012). Applications of fluorescence spectroscopy for predicting percent wastewater in an urban stream. *Environmental Science & Technology*, *46*(8), 4374-4381.

Groeneveld, M., Catalán, N., Attermeyer, K., Hawkes, J., Einarsdóttir, K., Kothawala, D., Bergquist, J., & Tranvik, L. (2020). Selective adsorption of terrestrial dissolved organic matter to inorganic surfaces along a boreal inland water continuum. *Journal of Geophysical Research: Biogeosciences*, *125*(3), e2019JG005236.

Gu, B., Schmitt, J., Chen, Z., Liang, L., & McCarthy, J. F. (1994). Adsorption and desorption of natural organic matter on iron oxide: mechanisms and models. *Environmental Science & Technology*, *28*(1), 38-46.

Guan, X.-H., Shang, C., & Chen, G.-H. (2006). Competitive adsorption of organic matter with phosphate on aluminum hydroxide. *Journal of Colloid and Interface Science*, *296*(1), 51-58.

Guggenberger, G., Zech, W., & Schulten, H.-R. (1994). Formation and mobilization pathways of dissolved organic matter: evidence from chemical structural studies of organic matter fractions in acid forest floor solutions. *Organic Geochemistry*, *21*(1), 51-66.

Guo, H., Li, X., Xiu, W., He, W., Cao, Y., Zhang, D., & Wang, A. (2019). Controls of organic matter bioreactivity on arsenic mobility in shallow aquifers of the Hetao Basin, PR China. *Journal of Hydrology*, *571*, 448-459.

Gustafsson, J. P. (2006). Arsenate adsorption to soils: Modelling the competition from humic substances. *Geoderma*, *136*(1-2), 320-330.

Gustafsson, J. P., Persson, I., Oromieh, A. G., van Schaik, J. W., Sjöstedt, C., & Kleja, D. B. (2014). Chromium (III) complexation to natural organic matter: mechanisms and modeling. *Environmental Science & Technology*, *48*(3), 1753-1761.

Haider, K. (2021). Problems related to the humification processes in soils of temperate climates. In *Soil biochemistry* (pp. 55-94). CRC Press.

Harvey, C., Ashfaque, K. N., Yu, W., Badruzzaman, A. B. M., Ali, M. A., Oates, P. M., Michael, H. A., Neumann, R. B., Beckie, R., Islam, S., & Ahmed, M. F. (2006). Groundwater dynamics and arsenic contamination in Bangladesh. *Chemical Geology*, *228*(1-3), 112-136. https://doi.org/10.1016/j.chemgeo.2005.11.025

Harvey, C., Swartz, C. H., Badruzzaman, A., Keon-Blute, N., Yu, W., Ali, M. A., Jay, J., Beckie, R., Niedan, V., & Brabander, D. (2002). Arsenic mobility and groundwater extraction in Bangladesh. *Science*, *298*(5598), 1602-1606.

Harvey, C., Swartz, C. H., Badruzzaman, A. B. M., Keon-Blute, N., Yu, W., Ali, M. A., Jay, J., Beckie, R., Niedan, V., & Brabander, D. (2005). Groundwater arsenic contamination on the Ganges Delta: biogeochemistry, hydrology, human perturbations, and human suffering on a large scale. *Comptes Rendus Geoscience*, *337*(1-2), 285-296.

Hasan, M. A., Ahmed, K. M., Sracek, O., Bhattacharya, P., Von Broemssen, M., Broms, S., Fogelström, J., Mazumder, M. L., & Jacks, G. (2007). Arsenic in shallow groundwater of Bangladesh: investigations from three different physiographic settings. *Hydrogeology Journal*, *15*(8), 1507-1522.

Hay, M. B., & Myneni, S. C. (2007). Structural environments of carboxyl groups in natural organic molecules from terrestrial systems. Part 1: Infrared spectroscopy. *Geochimica et Cosmochimica Acta*, *71*(14), 3518-3532.

Hayes, M. H., MacCarthy, P., Malcolm, R. L., & Swift, R. S. (1989). Humic substances II.

Haynes, R. (2005). Labile organic matter fractions as centralcomponents of the quality of agricultural soils: anoverview. *Adv Agron*, *5*, 221-268.

Horneman, A., van Geen, A., Kent, D. V., Mathe, P., Zheng, Y., Dhar, R., O'connell, S., Hoque, M., Aziz, Z., & Shamsudduha, M. (2004). Decoupling of As and Fe release to Bangladesh groundwater under reducing conditions. Part I: Evidence from sediment profiles. *Geochimica et Cosmochimica Acta*, *68*(17), 3459-3473.

Huang, Y., Knappett, P. S., Berube, M., Datta, S., Cardenas, M. B., Rhodes, K. A., Dimova, N. T., Choudhury, I., Ahmed, K. M., & van Geen, A. (2022). Mass fluxes of dissolved arsenic discharging to the

Meghna River are sufficient to account for the mass of arsenic in riverbank sediments. *Journal of Contaminant Hydrology*, *251*, 104068.

Huq, M. E., Fahad, S., Shao, Z., Sarven, M. S., Khan, I. A., Alam, M., Saeed, M., Ullah, H., Adnan, M., & Saud, S. (2020). Arsenic in a groundwater environment in Bangladesh: Occurrence and mobilization. *Journal of environmental management*, *262*, 110318.

Ilani, T., Schulz, E., & Chefetz, B. (2005). Interactions of organic compounds with wastewater dissolved organic matter: role of hydrophobic fractions. *Journal of environmental quality*, *34*(2), 552-562.

Jung, H. B., Bostick, B. C., & Zheng, Y. (2012). Field, experimental, and modeling study of arsenic partitioning across a redox transition in a Bangladesh aquifer. *Environ Sci Technol*, *46*(3), 1388-1395. https://doi.org/10.1021/es2032967

Jung, H. B., Charette, M. A., & Zheng, Y. (2009). Field, laboratory, and modeling study of reactive transport of groundwater arsenic in a coastal aquifer. *Environmental Science & Technology*, *43*(14), 5333-5338.

Jung, H. B., Zheng, Y., Rahman, M. W., Rahman, M. M., & Ahmed, K. M. (2015). Redox Zonation and Oscillation in the Hyporheic Zone of the Ganges-Brahmaputra-Meghna Delta: Implications for the Fate of Groundwater Arsenic during Discharge. *Appl Geochem*, *63*, 647-660. https://doi.org/10.1016/j.apgeochem.2015.09.001

Kaiser, K., & Guggenberger, G. (2007). Sorptive stabilization of organic matter by microporous goethite: sorption into small pores vs. surface complexation. *European Journal of Soil Science*, *58*(1), 45-59.

Kappler, A., Benz, M., Schink, B., & Brune, A. (2004). Electron shuttling via humic acids in microbial iron (III) reduction in a freshwater sediment. *FEMS microbiology ecology*, *47*(1), 85-92.

Kelleher, B. P., Simpson, M. J., & Simpson, A. J. (2006). Assessing the fate and transformation of plant residues in the terrestrial environment using HR-MAS NMR spectroscopy. *Geochimica et Cosmochimica Acta*, *70*(16), 4080-4094.

Kobayashi, T., & Sumida, H. (2015). Effects of humic acids on the sorption and bioavailability of pyrene and 1, 2-dihydroxynaphthalene. *Soil Science and Plant Nutrition*, *61*(sup1), 113-122.

Kulkarni, H. V., Mladenov, N., Datta, S., & Chatterjee, D. (2018a). Influence of monsoonal recharge on arsenic and dissolved organic matter in the Holocene and Pleistocene aquifers of the Bengal Basin. *Science of The Total Environment*, *637*, 588-599.

Kulkarni, H. V., Mladenov, N., Johannesson, K. H., & Datta, S. (2017). Contrasting dissolved organic matter quality in groundwater in Holocene and Pleistocene aquifers and implications for influencing arsenic mobility. *Applied geochemistry*, *77*, 194-205.

Kulkarni, H. V., Mladenov, N., McKnight, D. M., Zheng, Y., Kirk, M. F., & Nemergut, D. R. (2018b). Dissolved fulvic acids from a high arsenic aquifer shuttle electrons to enhance microbial iron reduction. *Science of The Total Environment*, *615*, 1390-1395.

Lalonde, K., Mucci, A., Ouellet, A., & Gélinas, Y. (2012). Preservation of organic matter in sediments promoted by iron. *Nature*, *483*(7388), 198-200.

Laspidou, C. S., & Rittmann, B. E. (2002). A unified theory for extracellular polymeric substances, soluble microbial products, and active and inert biomass. *water research*, *36*(11), 2711-2720.

Lee, D., & Seo, J. (2014). Three-dimensionally networked graphene hydroxide with giant pores and its application in supercapacitors. *Scientific reports*, *4*(1), 1-6.

Li, J., Wang, Y., Xie, X., Zhang, L., & Guo, W. (2013). Hydrogeochemistry of high iodine groundwater: a case study at the Datong Basin, northern China. *Environmental Science: Processes & Impacts*, *15*(4), 848-859.

Li, K., Khanna, R., Zhang, J., Barati, M., Liu, Z., Xu, T., Yang, T., & Sahajwalla, V. (2015). Comprehensive investigation of various structural features of bituminous coals using advanced analytical techniques. *Energy & fuels*, *29*(11), 7178-7189.

Li, Y., Gong, X., Sun, Y., Shu, Y., Niu, D., & Ye, H. (2022). High molecular weight fractions of dissolved organic matter (DOM) determined the adsorption and electron transfer capacity of DOM on iron minerals. *Chemical Geology*, *604*, 120907.

Lin, D., Pan, B., Zhu, L., & Xing, B. (2007). Characterization and phenanthrene sorption of tea leaf powders. *Journal of agricultural and food chemistry*, *55*(14), 5718-5724.

Lin, V. S. (2015). Research highlights: challenges in the characterization, storage, and isolation of natural organic matter. *Environmental Science: Processes & Impacts*, *17*(12), 2002-2005.

Litvin, V. A., & Minaev, B. F. (2013). Spectroscopy study of silver nanoparticles fabrication using synthetic humic substances and their antimicrobial activity. *Spectrochimica Acta Part A: Molecular and Biomolecular Spectroscopy*, *108*, 115-122.

Liu, G., Fernandez, A., & Cai, Y. (2011). Complexation of arsenite with humic acid in the presence of ferric iron. *Environmental Science & Technology*, *45*(8), 3210-3216.

Liu, K., Chen, Y., Xiao, N., Zheng, X., & Li, M. (2015). Effect of humic acids with different characteristics on fermentative short-chain fatty acids production from waste activated sludge. *Environmental Science & Technology*, *49*(8), 4929-4936.

Liu, R., Ma, T., Qiu, W., Du, Y., & Liu, Y. (2020a). Effects of Fe oxides on organic carbon variation in the evolution of clayey aquitard and environmental significance. *Science of The Total Environment*, *701*, 134776.

Liu, W., Wang, Y., Li, J., Qian, K., & Xie, X. (2020b). Indices of the dual roles of OM as electron donor and complexing compound involved in As and Fe mobilization in aquifer systems of the Datong Basin. *Environmental pollution*, *262*, 114305.

Liu, X., Lu, J., Fang, X., Zhou, J., & Chen, Q. (2022). Complexation modelling and oxidation mechanism of organic pollutants in cotton pulp black liquor during iron salt precipitation and electrochemical treatment. *Chemosphere*, *308*, 136374.

Lovley, D. R., Coates, J. D., Blunt-Harris, E. L., Phillips, E. J., & Woodward, J. C. (1996). Humic substances as electron acceptors for microbial respiration. *Nature*, *382*(6590), 445-448.

Lu, J., Shi, Y., Ji, Y., Kong, D., & Huang, Q. (2017). Transformation of triclosan by laccase catalyzed oxidation: The influence of humic acid-metal binding process. *Environmental pollution*, *220*, 1418-1423.

Lumsdon, D. G., & Fraser, A. R. (2005). Infrared spectroscopic evidence supporting heterogeneous site binding models for humic substances. *Environmental Science & Technology*, *39*(17), 6624-6631.

Lv, J., Han, R., Huang, Z., Luo, L., Cao, D., & Zhang, S. (2018). Relationship between molecular components and reducing capacities of humic substances. *ACS Earth and Space Chemistry*, *2*(4), 330-339.

Macalady, D. L., & Walton-Day, K. (2011). Redox chemistry and natural organic matter (NOM): Geochemists' dream, analytical chemists' nightmare. In *Aquatic redox chemistry* (pp. 85-111). ACS Publications.

MacCarthy, P., & Rice, J. A. (1985). Spectroscopic methods (other than NMR) for determining functionality in humic substances. *Humic substances in soil, sediment and water*, 527-559.

Mailloux, B. J., Trembath-Reichert, E., Cheung, J., Watson, M., Stute, M., Freyer, G. A., Ferguson, A. S., Ahmed, K. M., Alam, M. J., Buchholz, B. A., Thomas, J., Layton, A. C., Zheng, Y., Bostick, B. C., & van Geen, A. (2013). Advection of surface-derived organic carbon fuels microbial reduction in Bangladesh groundwater. *Proc Natl Acad Sci U S A*, *110*(14), 5331-5335. https://doi.org/10.1073/pnas.1213141110

Mayo, D. W., Miller, F. A., & Hannah, R. W. (2004). *Course notes on the interpretation of infrared and Raman spectra*.John Wiley & Sons.

McArthur, J., Banerjee, D., Hudson-Edwards, K., Mishra, R., Purohit, R., Ravenscroft, P., Cronin, A., Howarth, R., Chatterjee, A., & Talukder, T. (2004). Natural organic matter in sedimentary basins and its relation to arsenic in anoxic ground water: the example of West Bengal and its worldwide implications. *Applied geochemistry*, *19*(8), 1255-1293.

McArthur, J., Ravenscroft, P., Safiulla, S., & Thirlwall, M. (2001). Arsenic in groundwater: testing pollution mechanisms for sedimentary aquifers in Bangladesh. *Water Resources Research*, *37*(1), 109-117.

McClain, M. E., Boyer, E. W., Dent, C. L., Gergel, S. E., Grimm, N. B., Groffman, P. M., Hart, S. C., Harvey, J. W., Johnston, C. A., & Mayorga, E. (2003). Biogeochemical hot spots and hot moments at the interface of terrestrial and aquatic ecosystems. *Ecosystems*, 301-312.

McManus, J., Heinen, E. A., & Baehr, M. M. (2003). Hypolimnetic oxidation rates in Lake Superior: Role of dissolved organic material on the lake's carbon budget. *Limnology and Oceanography*, *48*(4), 1624-1632.

Mecozzi, M., & Pietrantonio, E. (2006). Carbohydrates proteins and lipids in fulvic and humic acids of sediments and its relationships with mucilaginous aggregates in the Italian seas. *Marine chemistry*, *101*(1-2), 27-39.

Mihajlov, I., Mozumder, M. R. H., Bostick, B. C., Stute, M., Mailloux, B. J., Knappett, P. S., Choudhury, I., Ahmed, K. M., Schlosser, P., & van Geen, A. (2020). Arsenic contamination of Bangladesh aquifers exacerbated by clay layers. *Nature communications*, *11*(1), 1-9.

Mikutta, C., & Kretzschmar, R. (2011). Spectroscopic evidence for ternary complex formation between arsenate and ferric iron complexes of humic substances. *Environmental Science & Technology*, *45*(22), 9550-9557.

Minor, E., & Stephens, B. (2008). Dissolved organic matter characteristics within the Lake Superior watershed. *Organic Geochemistry*, *39*(11), 1489-1501.

Minor, E. C., Swenson, M. M., Mattson, B. M., & Oyler, A. R. (2014). Structural characterization of dissolved organic matter: a review of current techniques for isolation and analysis. *Environmental Science: Processes & Impacts*, *16*(9), 2064-2079.

Mladenov, N., Zheng, Y., Miller, M. P., Nemergut, D. R., Legg, T., Simone, B., Hageman, C., Rahman, M. M., Ahmed, K. M., & McKnight, D. M. (2010). Dissolved organic matter sources and consequences for iron and arsenic mobilization in Bangladesh aquifers. *Environmental Science & Technology*, *44*(1), 123-128.

Mladenov, N., Zheng, Y., Simone, B., Bilinski, T. M., McKnight, D. M., Nemergut, D., Radloff, K. A., Rahman, M. M., & Ahmed, K. M. (2015). Dissolved organic matter quality in a shallow aquifer of Bangladesh: implications for arsenic mobility. *Environmental Science & Technology*, *49*(18), 10815-10824.

Mostofa, K. M., Liu, C.-q., Feng, X., Yoshioka, T., Vione, D., Pan, X., & Wu, F. (2013). Complexation of dissolved organic matter with trace metal ions in natural waters. In *Photobiogeochemistry of organic matter* (pp. 769-849). Springer.

Mukherjee, A., Fryar, A. E., & Howell, P. D. (2007a). Regional hydrostratigraphy and groundwater flow modeling in the arsenic-affected areas of the western Bengal basin, West Bengal, India. *Hydrogeology Journal*, *15*(7), 1397-1418.

Mukherjee, A., Fryar, A. E., & Rowe, H. D. (2007b). Regional-scale stable isotopic signatures of recharge and deep groundwater in the arsenic affected areas of West Bengal, India. *Journal of Hydrology*, *334*(1-2), 151-161.

Mukherjee, A. B., & Bhattacharya, P. (2001). Arsenic in groundwater in the Bengal Delta Plain: slow poisoning in Bangladesh. *Environmental Reviews*, *9*(3), 189-220.

Murphy, K. R., Stedmon, C. A., Graeber, D., & Bro, R. (2013). Fluorescence spectroscopy and multi-way techniques. PARAFAC. *Analytical Methods*, *5*(23), 6557-6566.

Neumann, R. B., Ashfaque, K. N., Badruzzaman, A., Ali, M. A., Shoemaker, J. K., & Harvey, C. F. (2010). Anthropogenic influences on groundwater arsenic concentrations in Bangladesh. *Nature Geoscience*, *3*(1), 46-52.

Neumann, R. B., Pracht, L. E., Polizzotto, M. L., Badruzzaman, A. B. M., & Ali, M. A. (2014). Biodegradable organic carbon in sediments of an arsenic-contaminated aquifer in Bangladesh. *Environmental Science & Technology Letters*, *1*(4), 221-225.

Ni, J., & Pignatello, J. J. (2018). Charge-assisted hydrogen bonding as a cohesive force in soil organic matter: water solubility enhancement by addition of simple carboxylic acids. *Environmental Science: Processes & Impacts*, *20*(9), 1225-1233.

Nicholas, S. L., Erickson, M. L., Woodruff, L. G., Knaeble, A. R., Marcus, M. A., Lynch, J. K., & Toner, B. M. (2017). Solid-phase arsenic speciation in aquifer sediments: A micro-X-ray absorption spectroscopy approach for quantifying trace-level speciation. *Geochimica et Cosmochimica Acta*, *211*, 228-255.

Nickson, R., McArthur, J., Burgess, W., Ahmed, K. M., Ravenscroft, P., & Rahmanñ, M. (1998). Arsenic poisoning of Bangladesh groundwater. *Nature*, *395*(6700), 338-338.

Nickson, R., McArthur, J., Ravenscroft, P., Burgess, W., & Ahmed, K. (2000). Mechanism of arsenic release to groundwater, Bangladesh and West Bengal. *Applied geochemistry*, *15*(4), 403-413.

Nogaro, G., Datry, T., Mermillod-Blondin, F., Foulquier, A., & Montuelle, B. (2013). Influence of hyporheic zone characteristics on the structure and activity of microbial assemblages. *Freshwater biology*, *58*(12), 2567-2583.

Nuzzo, A., Buurman, P., Cozzolino, V., Spaccini, R., & Piccolo, A. (2020). Infrared spectra of soil organic matter under a primary vegetation sequence. *Chemical and Biological Technologies in Agriculture*, *7*(1), 1-12.

Ohno, T. (2002). Fluorescence inner-filtering correction for determining the humification index of dissolved organic matter. *Environmental Science & Technology*, *36*(4), 742-746.

Olk, D., Brunetti, G., & Senesi, N. (2000). Decrease in humification of organic matter with intensified lowland rice cropping a wet chemical and spectroscopic investigation. *Soil Science Society of America Journal*, *64*(4), 1337-1347.

Omoike, A., Chorover, J., Kwon, K. D., & Kubicki, J. D. (2004). Adhesion of bacterial exopolymers to α-FeOOH: Inner-sphere complexation of phosphodiester groups. *Langmuir*, *20*(25), 11108-11114.

Oren, A., & Chefetz, B. (2012). Sorptive and desorptive fractionation of dissolved organic matter by mineral soil matrices. *Journal of environmental quality*, *41*(2), 526-533.

Pedrazas, M. N., Cardenas, M. B., Hosain, A., Demir, C., Ahmed, K. M., Akhter, S. H., Wang, L., Datta, S., & Knappett, P. S. (2021). Application of electrical resistivity to map the stratigraphy and salinity of fluvio-deltaic aquifers: case studies from Bangladesh that reveal benefits and pitfalls. *Hydrogeology Journal*, *29*(4), 1601-1610.

Peuravuori, J., & Pihlaja, K. (2004). Preliminary study of lake dissolved organic matter in light of nanoscale supramolecular assembly. *Environmental Science & Technology*, *38*(22), 5958-5967.

Piccolo, A. (1996). *Humic substances in terrestrial ecosystems*.Elsevier.

Pike, P. R., Sworan, P. A., & Cabaniss, S. E. (1993). Quantitative aqueous attenuated total reflectance Fourier transform infrared spectroscopy: Part II. Integrated molar absorptivities of alkyl carboxylates. *Analytica chimica acta*, *280*(2), 253-261.

Ping, C., Michaelson, G., Dai, X., & Candler, R. (2001). Characterization of soil organic matter. *Assessment methods for soil carbon*, 273-283.

Qiao, W., Guo, H., He, C., Shi, Q., Xiu, W., & Zhao, B. (2020). Molecular evidence of arsenic mobility linked to biodegradable organic matter. *Environmental Science & Technology*, *54*(12), 7280-7290.

Qiao, W., Guo, H., He, C., Shi, Q., & Zhao, B. (2021). Unraveling roles of dissolved organic matter in high arsenic groundwater based on molecular and optical signatures. *Journal of Hazardous Materials*, *406*, 124702.

Qu, S., & Cwiertny, D. M. (2013). Influence of organic surface coatings on the sorption of anticonvulsants on mineral surfaces. *Environmental Science: Processes & Impacts*, *15*(11), 2038-2049.

Ravenscroft, P., Burgess, W. G., Ahmed, K. M., Burren, M., & Perrin, J. (2005). Arsenic in groundwater of the Bengal Basin, Bangladesh: Distribution, field relations, and hydrogeological setting. *Hydrogeology Journal*, *13*(5), 727-751.

Reddy, S. B., Nagaraja, M., Kadalli, G., & Champa, B. (2018). Fourier transform infrared (FTIR) spectroscopy of soil humic and fulvic acids extracted from paddy land use system. *Int. J. Curr. Microbiol. Appl. Sci*, *7*, 834-837.

Redman, A. D., Macalady, D. L., & Ahmann, D. (2002). Natural organic matter affects arsenic speciation and sorption onto hematite. *Environmental Science & Technology*, *36*(13), 2889-2896.

Riedel, T., Zak, D., Biester, H., & Dittmar, T. (2013). Iron traps terrestrially derived dissolved organic matter at redox interfaces. *Proceedings of the National Academy of Sciences*, *110*(25), 10101-10105.

Sánchez-Monedero, M. A., Cegarra, J., García, D., & Roig, A. (2002). Chemical and structural evolution of humic acids during organic waste composting. *Biodegradation*, *13*(6), 361-371.

Sandron, S., Rojas, A., Wilson, R., Davies, N. W., Haddad, P. R., Shellie, R. A., Nesterenko, P. N., Kelleher, B. P., & Paull, B. (2015). Chromatographic methods for the isolation, separation and characterisation of dissolved organic matter. *Environmental Science: Processes & Impacts*, *17*(9), 1531-1567.

Schnitzer, M. (1983). Organic matter characterization. *Methods of Soil Analysis: Part 2 Chemical and Microbiological Properties*, *9*, 581-594.

Scott, D. T., McKnight, D. M., Blunt-Harris, E. L., Kolesar, S. E., & Lovley, D. R. (1998). Quinone moieties act as electron acceptors in the reduction of humic substances by humics-reducing microorganisms. *Environmental Science & Technology*, *32*(19), 2984-2989.

Senesi, N., D'orazio, V., & Ricca, G. (2003). Humic acids in the first generation of EUROSOILS. *Geoderma*, *116*(3-4), 325-344.

Sharma, P., Ofner, J., & Kappler, A. (2010). Formation of binary and ternary colloids and dissolved complexes of organic matter, Fe and As. *Environmental Science & Technology*, *44*(12), 4479-4485.

Shi, Z., Wang, P., Peng, L., Lin, Z., & Dang, Z. (2016). Kinetics of heavy metal dissociation from natural organic matter: roles of the carboxylic and phenolic sites. *Environmental Science & Technology*, *50*(19), 10476-10484.

Shuai, P., Cardenas, M. B., Knappett, P. S. K., Bennett, P. C., & Neilson, B. T. (2017a). Denitrification in the banks of fluctuating rivers: The effects of river stage amplitude, sediment hydraulic conductivity and dispersivity, and ambient groundwater flow. *Water Resources Research*, *53*(9), 7951-7967. https://doi.org/10.1002/2017wr020610

Shuai, P., Knappett, P. S., Hossain, S., Hosain, A., Rhodes, K., Ahmed, K. M., & Cardenas, M. B. (2017b). The impact of the degree of aquifer confinement and anisotropy on tidal pulse propagation. *Groundwater*, *55*(4), 519-531.

Simeoni, M. A., Batts, B. D., & McRae, C. (2003). Effect of groundwater fulvic acid on the adsorption of arsenate by ferrihydrite and gibbsite. *Applied geochemistry*, *18*(10), 1507-1515.

Smedley, P. L., & Kinniburgh, D. G. (2002). A review of the source, behaviour and distribution of arsenic in natural waters. *Applied geochemistry*, *17*(5), 517-568.

Smith, A. H., Lingas, E. O., & Rahman, M. (2000). Contamination of drinking-water by arsenic in Bangladesh: a public health emergency. *Bulletin of the World Health Organization*, *78*, 1093-1103.

Sposito, G. (2011). Electron shuttling by natural organic matter: twenty years after. In *Aquatic redox chemistry* (pp. 113-127). ACS Publications.

Stahl, M. O., Harvey, C. F., van Geen, A., Sun, J., Thi Kim Trang, P., Mai Lan, V., Mai Phuong, T., Hung Viet, P., & Bostick, B. C. (2016). River bank geomorphology controls groundwater arsenic concentrations in aquifers adjacent to the Red River, Hanoi Vietnam. *Water Resources Research*, *52*(8), 6321-6334.

Stevenson, F. J. (1994). *Humus chemistry: genesis, composition, reactions*.John Wiley & Sons.

Stüben, D., Berner, Z., Chandrasekharam, D., & Karmakar, J. (2003). Arsenic enrichment in groundwater of West Bengal, India: geochemical evidence for mobilization of As under reducing conditions. *Applied geochemistry*, *18*(9), 1417-1434.

Sun, K., Ran, Y., Yang, Y., & Xing, B. (2008). Sorption of phenanthrene by nonhydrolyzable organic matter from different size sediments. *Environmental Science & Technology*, *42*(6), 1961-1966.

Tang, J., & Weber, W. J. (2006). Development of engineered natural organic sorbents for environmental applications. 2. Sorption characteristics and capacities with respect to phenanthrene. *Environmental Science & Technology*, *40*(5), 1657-1663.

Tatzber, M., Stemmer, M., Spiegel, H., Katzlberger, C., Haberhauer, G., Mentler, A., & Gerzabek, M. H. (2007). FTIR-spectroscopic characterization of humic acids and humin fractions obtained by advanced NaOH, Na4P2O7, and Na2CO3 extraction procedures. *Journal of Plant Nutrition and Soil Science*, *170*(4), 522-529.

Thorn, K. A., Folan, D. W., & MacCarthy, P. (1989). Characterization of the International Humic Substances Society standard and reference fulvic and humic acids by solution state carbon-13 (13C) and hydrogen-1 (1H) nuclear magnetic resonance spectrometry. *Water-Resources Investigations Report*, *89*(4196), 1-93.

Tremblay, L., Kohl, S. D., Rice, J. A., & Gagné, J.-P. (2005). Effects of temperature, salinity, and dissolved humic substances on the sorption of polycyclic aromatic hydrocarbons to estuarine particles. *Marine chemistry*, *96*(1-2), 21-34.

van Geen, A., Ahmed, E. B., Pitcher, L., Mey, J. L., Ahsan, H., Graziano, J. H., & Ahmed, K. M. (2014). Comparison of two blanket surveys of arsenic in tubewells conducted 12 years apart in a 25 km(2) area of Bangladesh. *Sci Total Environ*, *488-489*, 484-492. https://doi.org/10.1016/j.scitotenv.2013.12.049

van Geen, A., Zheng, Y., Versteeg, R., Stute, M., Horneman, A., Dhar, R., Steckler, M., Gelman, A., Small, C., Ahsan, H., Graziano, J. H., Hussain, I., & Ahmed, K. M. (2003). Spatial variability of arsenic in 6000 tube wells in a 25 km2area of Bangladesh. *Water Resources Research*, *39*(5). https://doi.org/10.1029/2002wr001617

Varner, T. S., Kulkarni, H. V., Nguyen, W., Kwak, K., Cardenas, M. B., Knappett, P. S., Ojeda, A. S., Malina, N., Bhuiyan, M. U., & Ahmed, K. M. (2022). Contribution of sedimentary organic matter to arsenic mobilization along a potential natural reactive barrier (NRB) near a river: The Meghna river, Bangladesh. *Chemosphere*, *308*, 136289.

Vega, M. A., Kulkarni, H. V., Johannesson, K. H., Taylor, R. J., & Datta, S. (2020). Mobilization of co-occurring trace elements (CTEs) in arsenic contaminated aquifers in the Bengal basin. *Applied geochemistry*, *122*, 104709.

Vega, M. A., Kulkarni, H. V., Mladenov, N., Johannesson, K., Hettiarachchi, G. M., Bhattacharya, P., Kumar, N., Weeks, J., Galkaduwa, M., & Datta, S. (2017). Biogeochemical controls on the release and accumulation of Mn and As in shallow aquifers, West Bengal, India. *Frontiers in Environmental Science*, *5*, 29.

Wagai, R., & Mayer, L. M. (2007). Sorptive stabilization of organic matter in soils by hydrous iron oxides. *Geochimica et Cosmochimica Acta*, *71*(1), 25-35.

Wallace, G. C., Sander, M., Chin, Y.-P., & Arnold, W. A. (2017). Quantifying the electron donating capacities of sulfide and dissolved organic matter in sediment pore waters of wetlands. *Environmental Science: Processes & Impacts*, *19*(5), 758-767.

Wallis, I., Prommer, H., Berg, M., Siade, A. J., Sun, J., & Kipfer, R. (2020). The river–groundwater interface as a hotspot for arsenic release. *Nature Geoscience*, *13*(4), 288-295.

Waltham, C. A., & Eick, M. J. (2002). Kinetics of arsenic adsorption on goethite in the presence of sorbed silicic acid. *Soil Science Society of America Journal*, *66*(3), 818-825.

Wang, S., & Mulligan, C. N. (2006). Effect of natural organic matter on arsenic release from soils and sediments into groundwater. *Environmental geochemistry and health*, *28*(3), 197-214.

Wang, S., Wu, Y., An, J., Liang, D., Tian, L., Zhou, L., Wang, X., & Li, N. (2020). Geobacter autogenically secretes fulvic acid to facilitate the dissimilated iron reduction and vivianite recovery. *Environmental Science & Technology*, *54*(17), 10850-10858.

Weber Jr, W. J., McGinley, P. M., & Katz, L. E. (1992). A distributed reactivity model for sorption by soils and sediments. 1. Conceptual basis and equilibrium assessments. *Environmental Science & Technology*, *26*(10), 1955-1962.

Weinman, B., Goodbred, S. L., Zheng, Y., Aziz, Z., Steckler, M., van Geen, A., Singhvi, A. K., & Nagar, Y. C. (2008). Contributions of floodplain stratigraphy and evolution to the spatial patterns of groundwater arsenic in Araihazar, Bangladesh. *Geological Society of America Bulletin*, *120*(11-12), 1567-1580. https://doi.org/10.1130/b26209.1

Weishaar, J. L., Aiken, G. R., Bergamaschi, B. A., Fram, M. S., Fujii, R., & Mopper, K. (2003). Evaluation of specific ultraviolet absorbance as an indicator of the chemical composition and reactivity of dissolved organic carbon. *Environmental Science & Technology*, *37*(20), 4702-4708.

Wen, S., Lu, Y., Luo, C., An, S., Dai, J., Liu, Z., Zhong, J., & Du, Y. (2022). Adsorption of humic acids to lake sediments: Compositional fractionation, inhibitory effect of phosphate, and implications for lake eutrophication. *Journal of Hazardous Materials*, *433*, 128791.

Wu, R., Li, H., & Cao, P. (2009). Amelioration of weathered coal on soil physical, chemical properties and enzyme activities with vegetation restoration. *Journal of Agro-Environment Science*, *28*(9), 1855-1861.

Wu, X., Bowers, B., Kim, D., Lee, B., & Jun, Y.-S. (2019). Dissolved organic matter affects arsenic mobility and iron (III)(hydr) oxide formation: implications for managed aquifer recharge. *Environmental Science & Technology*, *53*(24), 14357-14367.

Xia, X., Teng, Y., & Zhai, Y. (2023). Influence of DOM and microbes on Fe biogeochemistry at a riverbank filtration site. *Environmental Research*, *216*, 114430.

Xue, Q., Ran, Y., Tan, Y., Peacock, C. L., & Du, H. (2019). Arsenite and arsenate binding to ferrihydrite organo-mineral coprecipitate: Implications for arsenic mobility and fate in natural environments. *Chemosphere*, *224*, 103-110.

Yamashita, Y., & Tanoue, E. (2003). Chemical characterization of protein-like fluorophores in DOM in relation to aromatic amino acids. *Marine chemistry*, *82*(3-4), 255-271.

Yi, X.-Y., Yang, Y.-P., Yuan, H.-Y., Chen, Z., Duan, G.-L., & Zhu, Y.-G. (2019). Coupling metabolisms of arsenic and iron with humic substances through microorganisms in paddy soil. *Journal of Hazardous Materials*, *373*, 591-599.

Yu, W. H., Harvey, C. M., & Harvey, C. F. (2003). Arsenic in groundwater in Bangladesh: A geostatistical and epidemiological framework for evaluating health effects and potential remedies. *Water Resources Research*, *39*(6).

Zhang, F., Li, X., Duan, L., Zhang, H., Gu, W., Yang, X., Li, J., He, S., Yu, J., & Ren, M. (2021). Effect of different DOM components on arsenate complexation in natural water. *Environmental pollution*, *270*, 116221.

Zhang, X., Sun, Y., Ma, F., Li, A., Zhao, H.-p., Wang, A., & Yang, J. (2019). In-situ utilization of soluble microbial product (SMP) cooperated with enhancing SMP-dependent denitrification in aerobic-anoxic sequencing batch reactor. *Science of The Total Environment*, *693*, 133558.

Zheng, Y., Stute, M., Van Geen, A., Gavrieli, I., Dhar, R., Simpson, H., Schlosser, P., & Ahmed, K. (2004). Redox control of arsenic mobilization in Bangladesh groundwater. *Applied geochemistry*, *19*(2), 201-214.

Zhu, A., Yang, Z., Liang, Z., Gao, L., Li, R., Hou, L., Li, S., Xie, Z., Wu, Y., & Chen, J. (2020). Integrating hydrochemical and biological approaches to investigate the surface water and groundwater interactions in the hyporheic zone of the Liuxi River basin, southern China. *Journal of Hydrology*, *583*, 124622.

Zsolnay, Á. (2003). Dissolved organic matter: artefacts, definitions, and functions. *Geoderma*, *113*(3-4), 187-209.